





Small-Molecule Mn Antioxidants in *Caenorhabditis elegans* and *Deinococcus radiodurans* Supplant MnSOD Enzymes during Aging and Irradiation

Elena K. Gaidamakova,^{a,b} Ajay Sharma,^{c,d} Vera Y. Matrosova,^{a,b} Olga Grichenko,^{a,b} Robert P. Volpe,^{a,b} Rok Tkavc,^{a,b,n} Isabel H. Conze,^{a,e,f} Polina Klimentkova,^{a,b} Irina Balygina,^{a,g} William H. Horne,^{a,h}  Cene Gostinčar,ⁱ Xiao Chen,^j Kira S. Makarova,^k Igor Shuryak,^l Chandra Srinivasan,^m Belinda Jackson-Thompson,^{a,b} Brian M. Hoffman,^{c,d}  Michael J. Daly^a

^aDepartment of Pathology, School of Medicine, Uniformed Services University of the Health Sciences (USUHS), Bethesda, Maryland, USA

^bHenry M. Jackson Foundation for the Advancement of Military Medicine, Bethesda, Maryland, USA

^cDepartment of Chemistry, Northwestern University, Evanston, Illinois, USA

^dDepartment of Molecular Biosciences, Northwestern University, Evanston, Illinois, USA

^eCologne Excellence Cluster on Cellular Stress Responses in Aging-Associated Diseases (CECAD), University of Cologne, Cologne, Germany

^fInstitute for Genetics, University of Cologne, Cologne, Germany

^gNovosibirsk State University, Novosibirsk, Russia

^hDepartment of Chemistry and Life Science, United States Military Academy, West Point, New York, USA

ⁱDepartment of Biology, University of Ljubljana, Biotechnical Faculty, Ljubljana, Slovenia

^jJGM Biosciences, Mountain View, California, USA

^kNational Center for Biotechnology Information, National Library of Medicine, National Institutes of Health, Bethesda, Maryland, USA

^lCenter for Radiological Research, Columbia University Irving Medical Center, New York, New York, USA

^mDepartment of Chemistry & Biochemistry, California State University, Dominguez Hills, California, USA

ⁿDepartment of Microbiology and Immunology, School of Medicine, Uniformed Services University of the Health Sciences (USUHS), Bethesda, Maryland, USA

Elena K. Gaidamakova, Ajay Sharma, and Vera Y. Matrosova contributed equally. Author order was determined by agreement. Michael J. Daly and Brian M. Hoffman contributed equally to writing this report.

ABSTRACT Denham Harman's oxidative damage theory identifies superoxide ($O_2^{\bullet-}$) radicals as central agents of aging and radiation injury, with Mn²⁺-dependent superoxide dismutase (MnSOD) as the principal $O_2^{\bullet-}$ -scavenger. However, in the radiation-resistant nematode *Caenorhabditis elegans*, the mitochondrial antioxidant enzyme MnSOD is dispensable for longevity, and in the model bacterium *Deinococcus radiodurans*, it is dispensable for radiation resistance. Many radiation-resistant organisms accumulate small-molecule Mn²⁺-antioxidant complexes well-known for their catalytic ability to scavenge $O_2^{\bullet-}$, along with MnSOD, as exemplified by *D. radiodurans*. Here, we report experiments that relate the MnSOD and Mn-antioxidant content to aging and oxidative stress resistances and which indicate that *C. elegans*, like *D. radiodurans*, may rely on Mn-antioxidant complexes as the primary defense against reactive oxygen species (ROS). Wild-type and Δ MnSOD *D. radiodurans* and *C. elegans* were monitored for gamma radiation sensitivities over their life spans while gauging Mn²⁺-antioxidant content by electron paramagnetic resonance (EPR) spectroscopy, a powerful new approach to determining the *in vivo* Mn-antioxidant content of cells as they age. As with *D. radiodurans*, MnSOD is dispensable for radiation survivability in *C. elegans*, which hyperaccumulates Mn-antioxidants exceptionally protective of proteins. Unexpectedly, Δ MnSOD mutants of both the nematodes and bacteria exhibited increased gamma radiation survival compared to the wild-type. In contrast, the loss of MnSOD renders radiation-resistant bacteria sensitive to atmospheric oxygen during desiccation. Our results support the concept that the disparate responses to oxidative stress are explained by the accumulation of Mn-antioxidant complexes which protect, complement, and can even supplant MnSOD.

Editor Michael David Leslie Johnson, University of Arizona

This is a work of the U.S. Government and is not subject to copyright protection in the United States. Foreign copyrights may apply.

Address correspondence to Brian M. Hoffman, bmh@northwestern.edu, or Michael J. Daly, michael.daly@usuhs.edu.

The authors declare no conflict of interest.

This article is a direct contribution from Kira S. Makarova, a Fellow of the American Academy of Microbiology, who arranged for and secured reviews by Dea Slade, Max Perutz Labs, University of Vienna, and Victoria DeRose, University of Oregon.

Received 10 November 2021

Accepted 28 November 2021

Published 11 January 2022

IMPORTANCE The current theory of cellular defense against oxidative damage identifies antioxidant enzymes as primary defenders against ROS, with MnSOD being the preeminent superoxide ($O_2^{\bullet-}$) scavenger. However, MnSOD is shown to be dispensable both for radiation resistance and longevity in model organisms, the bacterium *Deinococcus radiodurans* and the nematode *Caenorhabditis elegans*. Measured by electron paramagnetic resonance (EPR) spectroscopy, small-molecule Mn-antioxidant content was shown to decline in unison with age-related decreases in cell proliferation and radioresistance, which again are independent of MnSOD presence. Most notably, the Mn-antioxidant content of *C. elegans* drops precipitously in the last third of its life span, which links with reports that the steady-state level of oxidized proteins increases exponentially during the last third of the life span in animals. This leads us to propose that global responses to oxidative stress must be understood through an extended theory that includes small-molecule Mn-antioxidants as potent $O_2^{\bullet-}$ -scavengers that complement, and can even supplant, MnSOD.

KEYWORDS ionizing radiation, aging, desiccation, ROS, Mn antioxidants, MnSOD, EPR, *Deinococcus*, *Caenorhabditis*, *Lactobacillus*, reactive oxygen species, superoxide dismutase

In the current Denham Harman oxidative damage theory, antioxidant enzymes defend against reactive oxygen species (ROS) that contribute to aging and radiosensitivity, with Mn-dependent superoxide dismutase (MnSOD) being the central superoxide ($O_2^{\bullet-}$) scavenger (1–3). Here, we report tests of the hypothesis that this theory must be broadened to incorporate an additional major defense mechanism, small-molecule Mn-antioxidant complexes (denoted H-Mn). To begin, MnSOD has been shown to be dispensable both for longevity and radiation resistance in several model prokaryotes, fungi, and simple animals (3–5). Building on these findings, we apply a new spectroscopic approach to measure cellular Mn antioxidant content and integrate our present findings with the previous studies. The result is a broadened picture of cellular defense against the oxidative stress caused by the diverse mechanisms of $O_2^{\bullet-}$ formation.

Focusing first on radiation resistance, the model bacterium *Deinococcus radiodurans* typically survives after 10 kGy of acute gamma radiation and grows luxuriantly under chronic ionizing radiation (60 Gy/h). However, MnSOD was shown to be dispensable for such radiation resistance in several prokaryotes, including *D. radiodurans*, and in some fungi (4–6).

There is a well-established linkage between radiation resistance and aging. It has been found that in all known cell types, the age at the time of radiation exposure is one of the principal factors controlling radiation-induced cell injury. Resistance typically increases until maturity but then declines through senescence until death (7–9). The short-lived nematode model organism *Caenorhabditis elegans*, which is extremely resistant to ionizing radiation, has been used to critically examine aging. Adults can survive 1,000 Gy with unaltered life spans (10). However, by manipulating expression of the *C. elegans* genes encoding its five SOD isoforms, it was found that the absence of MnSOD or CuZnSOD has little, if any, effect on the life span of *C. elegans*. As these results contradicted the view that SOD enzymes are the primary defense against ROS-induced aging, they led to the surprising conclusion that $O_2^{\bullet-}$ is not a major determinant of aging in this model organism (11).

However, cellular defenses against $O_2^{\bullet-}$ are more diverse than these considerations recognize. In desiccation- and radiation-resistant species of archaea, bacteria, and yeasts (12, 13) Mn is present not only as MnSOD, but also in a nonenzymatic form as low-molecular-weight H-Mn²⁺ complexes with accumulated metabolites (e.g., carboxylic acids, amino acids, peptides, nucleosides, orthophosphate) that exhibit catalytic ROS scavenging (5, 14–19) (Text S1). In particular, studies have revealed the exceptional efficacy of such small-molecule Mn antioxidants in protecting proteins against oxidative damage (20, 21). Indeed, rationally designed *Deinococcus* Mn²⁺-peptide antioxidants are now used as radioprotectants in the production of irradiated vaccines (22–25).

As radiation and desiccation resistance and aging all are tied to the deleterious influences of $O_2^{\bullet-}$, in this introduction we first briefly review aspects of the role of Mn in $O_2^{\bullet-}$ defense, both Mn in the enzymatic form as MnSOD and as small-molecule Mn-antioxidant

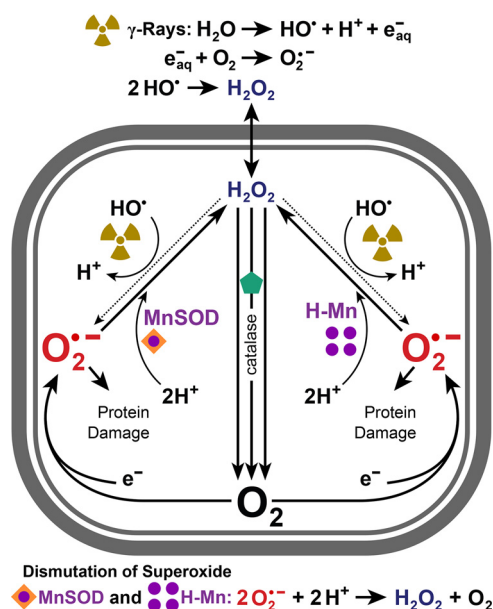


FIG 1 Ionizing radiation-driven reactions related to dismutation of superoxide by MnSOD and Mn antioxidants, illustrating the two complementary catalysts of superoxide defense, MnSOD and Mn antioxidants (H-Mn).

complexes. We then extend this to the linkage between radiation resistance, desiccation resistance, and aging, and the consequences of the presence or absence of MnSOD and Mn antioxidants, which is a focus of the analytical approach described in this report.

Mn and resistance to superoxide. Mn^{2+} ions are unique among redox-active transition metals that accumulate in cells in that they are innocuous under conditions where other biologically active transition metals (in particular, Fe^{2+}) tend to promote formation of ROS (26). Therefore, cells and their organelles can accumulate up to millimolar concentrations of Mn^{2+} ions in the form of Mn^{2+} -metabolite complexes (Mn antioxidants), along with MnSOD (13, 16, 27). Both MnSOD and Mn antioxidants catalytically scavenge $\text{O}_2^{\bullet-}$ formed through metabolic processes or by radiation exposure, converting these ions to hydrogen peroxide (H_2O_2) (20, 28, 29) (Fig. 1). H_2O_2 is membrane-permeable and can escape the cell (20); in contrast, $\text{O}_2^{\bullet-}$ is not membrane-permeable and becomes trapped and accumulates in cells (30). Without these Mn-mediated means of eliminating $\text{O}_2^{\bullet-}$, the $\text{O}_2^{\bullet-}$ radicals can directly react with certain amino acids and Fe-S groups of proteins or can further react to form hydroxyl (HO^\bullet) radicals that cause indiscriminate proteome and genome damage, which in turn lead to disruption of protein homeostasis and DNA repair malfunction (20, 21, 31–34) (Fig. 1).

The importance of Mn antioxidants extends beyond radiation survival. Deinococci are nonsporulating obligate aerobes and are further renowned for their desiccation resistance (12), a Mn-dependent metabolic trait associated with proteome protection under atmospheric O_2 (35). Whereas $\text{O}_2^{\bullet-}$ in desiccating cells is derived mostly from atmospheric O_2 , $\text{O}_2^{\bullet-}$ in irradiated cells is also formed by radiolytic reduction of O_2 released through the intracellular decomposition of ionizing radiation-generated H_2O_2 as catalyzed by enzymes (e.g., catalase) (Fig. 1) (20, 26). Mounting evidence supports the hypothesis that ionizing radiation resistance is simply a secondary phenotype that accompanies resistance to other more commonly encountered environmental stressors, particularly the hyperoxic conditions during cycles of exposure to atmospheric O_2 during desiccation and subsequent rehydration (12, 35).

The present study. Both *D. radiodurans* and *C. elegans* are known for their extreme radiation resistance. However, MnSOD is found to be dispensable for radiation protection, a finding that contradicts the view of cellular defense against oxidative stress that implicates MnSOD as the dominant protection against ROS. Thus, these organisms are

models for study to identify the roles of Mn antioxidants and MnSOD in protection against various sources of oxidative stress.

In this report, we tracked the gamma radiation survival of *D. radiodurans* bacteria and *C. elegans* nematodes throughout their life span. In this effort, we controlled MnSOD content by mutation while probing Mn²⁺ speciation and coordination of Mn antioxidants by electron paramagnetic resonance (EPR) spectroscopy. Prior to the use of EPR, there was no means of determining Mn²⁺ antioxidant content *in vivo*. Standard analytical procedures that disrupt cells alter the chemical speciation of Mn²⁺, thus destroying information about the *in vivo* properties. In contrast, EPR methodologies, namely, EPR, ENDOR, and ESEEM spectroscopies, directly characterize the speciation of Mn²⁺ *in vivo*. We previously used EPR to show that radiation-resistant cell-types possess a high population of Mn antioxidant complexes and are readily distinguishable from radiation-sensitive cell types that lack Mn antioxidants (5, 36). We showed that radiation resistance correlates directly with cellular concentrations of Mn antioxidants (5, 15, 20, 26) and extended this here to include the model bacterium *Lactobacillus plantarum*, which does not encode SODs but hyperaccumulates Mn antioxidants (37–39).

This study enables us to consider paradoxes and puzzles in Denham Harman's oxidative damage theory viewed from the perspective of three extremely radiation-resistant model organisms—*C. elegans*, *D. radiodurans*, and *L. plantarum*. We evaluated the variations in MnSOD and H-Mn antioxidant content with aging and oxidative stress resistances, and formulate an extended theory of oxidative stress defense in which small-molecule Mn antioxidants are complementary to MnSOD, and in some cases can supplant MnSOD, in O₂^{•-}-scavenging.

RESULTS

We begin by showing (in the following subsection) that cellular Mn antioxidant content in *D. radiodurans* can be manipulated by aging and is independent of the presence of MnSOD. Next, it is shown that the same is true for *C. elegans*. However, it is finally shown (in the section "*D. radiodurans* and *L. plantarum* become desiccation-sensitive upon loss of MnSOD") that MnSOD is nonetheless required for defense against the oxidative stress of desiccation in bacteria, as it is for defense against chemical agents such as paraquat.

Mn antioxidant content and gamma radiation resistance decrease in unison with age in *D. radiodurans*, independent of the presence of MnSOD. The chronological life span of *D. radiodurans* is measured here as the time a cell survives in a nonreplicating (stationary) state, with survival being defined as the ability to form a colony on fresh medium. The effect of aging on wild-type (WT) and Δ MnSOD cultures is characterized by measuring the decrease in radiation survival with time of the stationary-phase cultures (Fig. 2A and B), and in cellular Mn antioxidant content as determined by EPR (Fig. 2C and D). The experiments began by inoculating mid-exponential-phase WT (ATCC BAA-816) and *sodA*⁻ (Δ MnSOD) cells into separate Erlenmeyer flasks with 0.8 L liquid TGY (1% bactotryptone, 0.5% yeast extract, and 0.1% glucose). These cultures were followed during incubation with agitation at 32°C for up to 10 days without change of broth (Fig. 2A, B and F; see also replicate study Fig. S1A, D, and E).

Over the 10-day study, we measured cell survival and gamma radiation resistance during aging, which are measures of replicative fitness, by use of the CFU assay. We show that young and mature WT and *sodA*⁻ cells are similarly resistant to 10 kGy and that they become progressively less resistant as they grow older (Fig. 2A and B). Unexpectedly, the *sodA*⁻ strain displayed even greater radiation resistance and longevity compared to the WT (Fig. 2B; see also Fig. S1D and E). This can be explained by delayed growth of the *sodA*⁻ mutant (Fig. 2F; see also Fig. S1A), which would conserve metabolites needed for radiation survival (40); however, other explanations are equally plausible (see Discussion).

In parallel, we employed EPR spectroscopy to measure the content of Mn antioxidants, which is a ruler of cellular radiation resistance (5). We collected 35-GHz continuous-wave (CW) absorption-display EPR spectra for WT and *sodA*⁻ *D. radiodurans* cells harvested at days 1, 2, 6, and 10 (Fig. 2C and D; see also Fig. S1B and C). We had previously shown that such absorption-display EPR spectra at X- or Q-bands, but not derivative-display spectra, reveal that

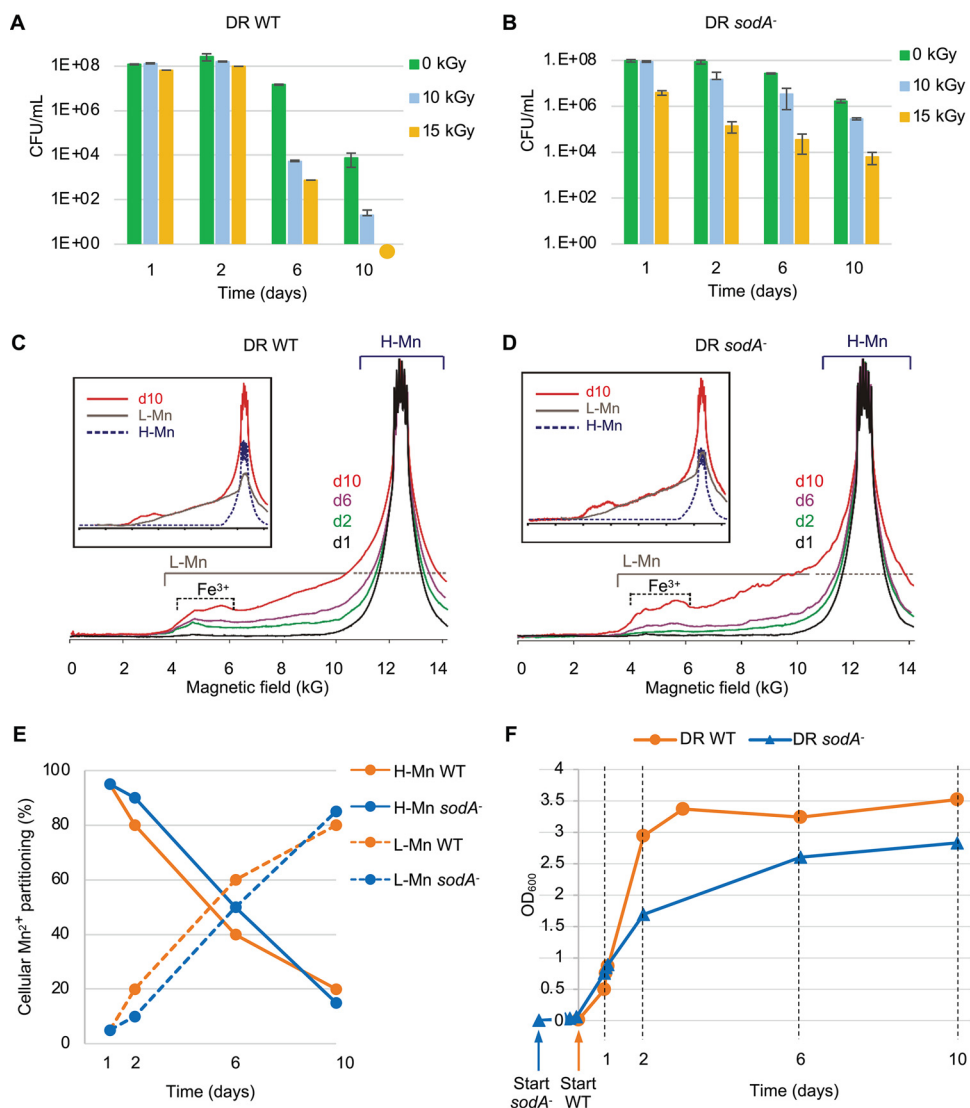


FIG 2 Gamma radiation survival and H-Mn content over the life span of *D. radiodurans*. (A) WT survival (CFU/mL) of young (day 1 [d1]), mature (d2), old (d6), and dying (d10) *D. radiodurans* (DR) cells exposed to 0, 10, and 15 kGy (⁶⁰Co) (replicate, Fig. S1D). (B) Δ MnSOD (*sodA*⁻) survival as in panel A (replicate, Fig. S1E). (C) Normalized EPR spectra of WT cells of panel A showing a relative increase with aging in the intensity of the broad wings, associated with L-Mn relative to the normalized intensity of the narrow response from H-Mn. (Inset) Partition of cellular Mn²⁺ into two pools, H-Mn (Mn antioxidants) and L-Mn (Mn-proteins) for day-10 cells (see Fig. S2, which shows the partition of cellular Mn²⁺ into H-Mn/L-Mn for all cell-types). (D) EPR spectra for *sodA*⁻ cells of panel B with aging. (Inset) Partition of cellular Mn²⁺ into H-Mn and L-Mn for day-10 cells. (E) Changes in fractions of cellular H-Mn and L-Mn complexes in WT and *sodA*⁻ with bacterial aging, as deduced from decompositions of EPR spectra (see Fig. S2). For details of the procedures for quantifying H-Mn and L-Mn contributions, see reference 5. (F) Δ MnSOD-induced growth lag in cultures (replicate, Fig. S1A).

cellular Mn²⁺ exists as two distinct pools of Mn²⁺ complexes, denoted H-Mn and L-Mn (5, 41). The H-Mn spectrum is centered around an \sim 12-kG magnetic field and is dominated by a relatively narrow Mn²⁺ signal (\sim 1.5 kG half-max width) that displays a sextet pattern arising from hyperfine interactions with the ⁵⁵Mn (nuclear spin, $I = 5/2$) nucleus (hyperfine coupling, $A \sim$ 90 G) (5, 36, 41) and arises from the high-symmetry, cellular small-molecule Mn antioxidant complexes (H-Mn, for example; these include Mn²⁺ complexed with orthophosphate [Pi] and peptides). The H-Mn spectrum may “ride on” and be flanked by broad “wings” extending from low fields, \sim 3 kG, to higher fields well beyond the magnet limit. These features are associated with a heterogeneous population of low-symmetry Mn²⁺-bound complexes and enzymes denoted L-Mn (41). The fractional contributions from H-Mn and L-Mn

populations to the Mn^{2+} EPR spectra are shown in Fig. 2E, as calculated using the protocol described previously (5).

Comparison of the EPR spectra of young, mature, and old WT and $\Delta MnSOD$ *D. radiodurans* cells showed that life stage and radiation resistance track with the population of H-Mn complexes, but not with MnSOD content (Fig. 2C and D). Specifically, young (day 1 [d1]) *D. radiodurans* cells contain almost exclusively Mn^{2+} in antioxidant H-Mn complexes (Fig. 2E), characteristic of high radiation resistance. As cells senesce (d2 to d10), their EPR spectra progressively display increasingly intense wings derived from L-Mn complexes characteristic of radiation-sensitive organisms (5) (Fig. 2C and D; see also Fig. S1B and C), as the fraction of H-Mn decreases and that of L-Mn increases (Fig. 2E). Correspondingly, the radiation resistance decreases track with the fraction of H-Mn (Fig. 2A and B). Of particular importance, as noted above, radiation resistance is not merely undiminished by elimination of MnSOD in the *sodA*⁻ strain, but in fact, the resistance of the strain is somewhat greater than that of WT during aging.

As gauged by EPR, Mn-antioxidant content decreases in unison with age in *C. elegans*, independent of the presence of MnSOD. Similar to *D. radiodurans*, the life span of *C. elegans* is reported to be unaffected or even somewhat increased in $\Delta MnSOD$ mutants (11, 42, 43) (Fig. 2A and B). As we now show in Fig. 3, *C. elegans* nematodes also display the two important molecular hallmarks seen for radiation-resistant microorganisms: (i) an extremely high H-Mn content and near-absence of L-Mn as measured by Mn^{2+} EPR, in contrast to radiation-sensitive organisms (5) (Fig. 3A), and (ii) as correspondingly measured analytically, a high cellular concentration of small-molecule $O_2^{\bullet-}$ -scavenging Mn antioxidants that protect proteins (15, 20, 22–24, 44, 45) (Fig. 3F and G).

In relation to item (i), above, Fig. 3A shows the absorption-display EPR spectra of young (d2) *C. elegans* WT (N2) and *sod* deletion mutants (inset); *sod-1,2,3,4,5* (ΔSOD) is a quintuple mutant with complete loss of MnSOD and Cu/ZnSOD activities; *sod-2,3* is a double mutant deficient in MnSOD enzymes ($\Delta MnSOD$); *sod-2* and *sod-3* are single $\Delta MnSOD$ mutants (43, 46). Included for comparison are the EPR spectra of the radiation-resistant bacterium *L. plantarum* (5, 37, 38, 47) and two radiation-sensitive species, the bacterium *Escherichia coli* K-12 and the yeast *Saccharomyces cerevisiae* EXF-6218 (5). The EPR spectra of all the young nematodes (WT and the four *sod* knockout mutants; see inset of Fig. 3A) show that the Mn^{2+} is almost exclusively present as H-Mn, with a negligible contribution from L-Mn, and likewise for *L. plantarum*. This contrasts with the EPR spectra of radiation-sensitive *E. coli* K-12 and *S. cerevisiae* EXF-6218 (mature, healthy cells), which are dominated by a large pool of L-Mn that generates the intense wings of the spectra, with only a small pool of H-Mn.

The first important result from Fig. 3 is that EPR shows that *C. elegans* hyperaccumulates H-Mn, with H-Mn content undiminished for all SOD knockout strains compared to WT (Fig. 3A). We next compared aging WT and $\Delta MnSOD$ nematode populations and focused on their Mn antioxidant content before and after the onset of senescence, as characterized by increasingly sluggish, nonmotile, and unresponsive worm behaviors, which are measures of metabolic fitness. The nematodes were monitored for survival over 3 to 4 weeks, displaying the following stages: young worms (d1 to d3), mature (middle-aged) worms (d5 to d13), old worms (d15 to d21), and dead worms (>d26). Analogous to aging *D. radiodurans* bacteria (Fig. 2C), the normalized EPR spectra for WT nematodes exhibited an age-dependent loss of H-Mn antioxidant content over the life span (Fig. 3B); EPR spectra show that young and mature worms (inset) contain only H-Mn, whereas H-Mn decreases as L-Mn increases in older worms (Fig. 3E). As a follow-up to this primary study (Fig. 3B), we grew WT and $\Delta MnSOD$ in parallel and harvested worms at d2 (young), d7 (mature), and d18 (old), and collected their EPR spectra (Fig. 3C and D). Consistent with *D. radiodurans*, the young and mature worms displayed very high H-Mn antioxidant levels, with a loss in H-Mn antioxidant content and an increase in L-Mn in the older worms (Fig. 3C and D; see also Fig. S3). Moreover, at the various stages of aging, the H-Mn population is unchanged in $\Delta MnSOD$ *C. elegans* compared to WT (Fig. 3C and D; see also Fig. S3), as is the case with *D. radiodurans*.

In relation to item (ii), above, the small-molecule antioxidant capacity of *C. elegans* was directly confirmed using aqueous-phase extracts of WT (d2) homogenates, which were first subjected to ultracentrifugation and then to ultrafiltration. Ultracentrifugation removed

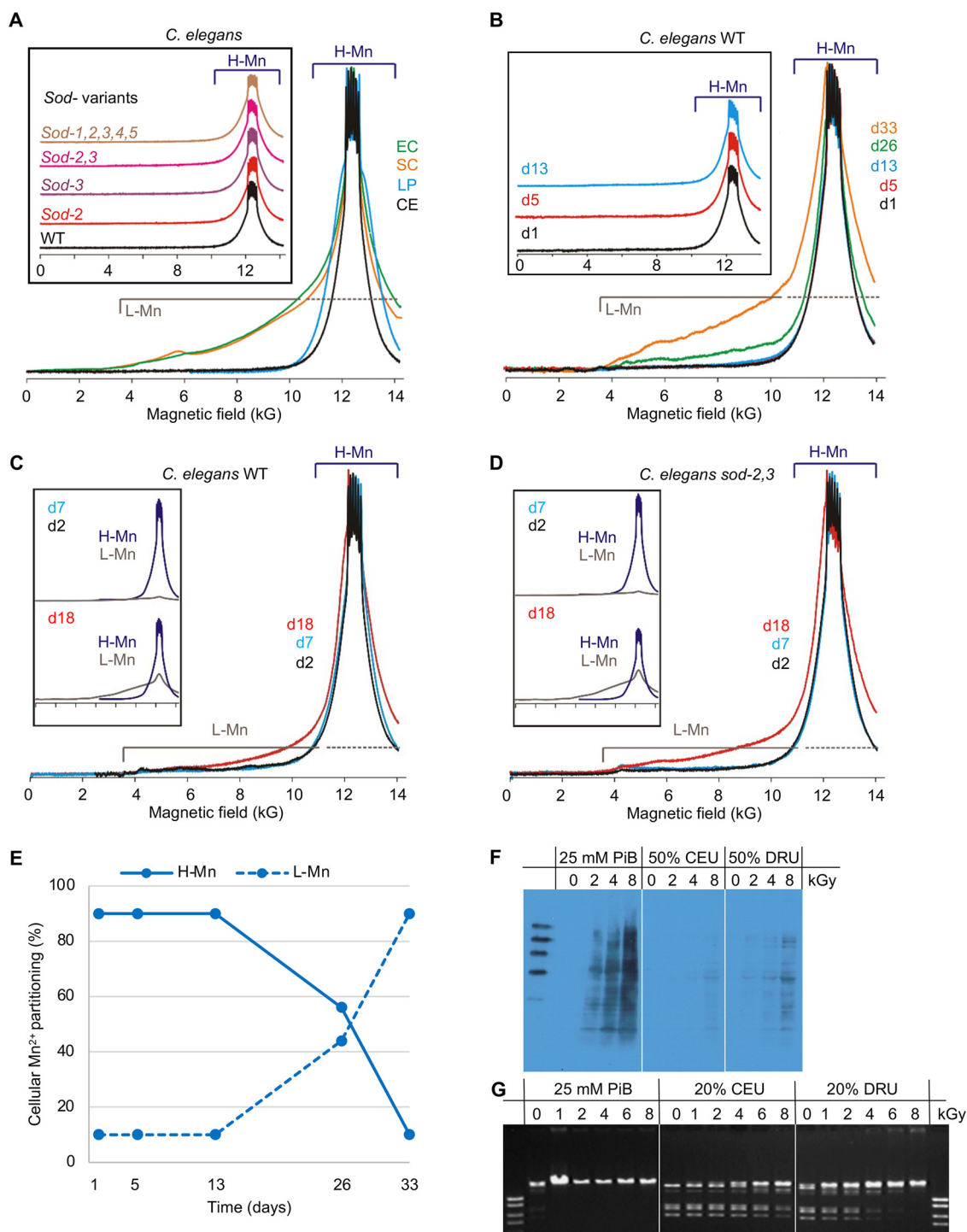


FIG 3 Mn antioxidant content of *C. elegans* and their small-molecule extracts. (A) Normalized EPR spectra of radiation-resistant young (d2) WT (N2) and Δ SOD mutant nematodes (CE) (see inset), dominated by H-Mn, plus the radiation-resistant *L. plantarum* (LP), compared to the two naturally radiosensitive species, *E. coli* K-12 (EC) and *S. cerevisiae* (SC) EXF-6218, which show the strong wings associated with L-Mn in young (d1) cells. (B) Normalized EPR spectra of WT nematodes across their life span; d1 (young), d5 (mature), d13 (mature), d26 (old, sluggish, and nonresponsive), and d33 (dead) displaying a relative increase in intensity of the broad wings, associated with L-Mn compared to the intensity of the narrow response from H-Mn with aging. (C) EPR spectra of WT nematodes (d2, d7, d18). (Inset) Partition of cellular Mn^{2+} into H-Mn and L-Mn pools. (D) EPR spectra of *sod-2,3* (Δ MnSOD) nematodes (d2, d7, d18). (Inset) Partition of cellular Mn^{2+} into H-Mn and L-Mn. (E) Changes in fractions of cellular H-Mn and L-Mn complexes in WT nematodes with aging, as deduced from decompositions of EPR spectra (panel B). For details of the procedures for quantifying H-Mn and L-Mn contributions, see reference 5. (F) CEU (*C. elegans* ultrafiltrate) of WT (d2) nematodes protects irradiated proteins. CEU was mixed with purified *E. coli* proteins and exposed to the indicated doses of gamma rays (kGy). Irradiated proteins were then separated by polyacrylamide gel electrophoresis, and protein oxidation was visualized by Western (Continued on next page)

proteins and other macromolecules and peptides greater than 1 kDa. As a precaution, the ultracentrifuged supernatants were also ultrafiltered to remove any contaminating molecules (>3 kDa) released from the pellets during collection of the supernatants.

When WT *C. elegans* ultrafiltrates were mixed with proteins purified from *E. coli* and exposed to gamma radiation, high levels of protein protection were indicated by Western blotting carbonyl analysis (Fig. 3F); carbonyl groups are the most widely used marker of irreversible protein oxidation (15, 20, 31, 48–51). Side-by-side comparisons showed that *C. elegans* ultrafiltrate (CEU) was even more radioprotective than *D. radiodurans* ultrafiltrate (DRU), which is highly enriched in small-molecule Mn complexes (15). At 4,000 Gy of gamma rays, for proteins mixed with PiB alone, proteins were heavily oxidized (carbonylated) as visualized through blacking in the Western blots. In stark contrast, when the *E. coli* proteins were irradiated in the presence of CEU, there was no significant protein carbonylation (Fig. 3F).

We also tested the ability of CEU to protect the activity of the restriction endonuclease BamHI, a radiation-sensitive enzyme inactivated *in vitro* by ~150 Gy (15). Whereas diluted DRU protected the *in vitro* activity of BamHI to 4,000 Gy, an equivalent amount of CEU protected the enzyme to 8,000 Gy (Fig. 3G). Thus, *C. elegans* cells have an even greater antioxidant capacity than the most radioresistant bacteria, *D. radiodurans* (20).

ΔSOD (sod-1,2,3,4,5) *C. elegans* outlives WT under intense gamma irradiation.

Longevity in this study represents the ability of nematodes to maintain healthy (active, motile, responsive) behaviors under high-level chronic radiation, in physiological conditions where nematodes are metabolically active but cannot proliferate, as fecundity is the earliest major function lost to irradiation. Reproductive sterilization is reported at doses as low as 500 Gy (10), and consistently, we did not see proliferation of nematodes growing under chronic irradiation. Taking the major endpoint as survival of individual animals, we studied the effect on the activity and life span of groups of 40 adult nematodes on strain OP50 plates incubated under 34.75 Gy/h over 8 days (Fig. 4A).

The Kaplan-Meier survival curves for chronically irradiated WT and ΔSOD *C. elegans* strains are shown (Fig. 4A; see also Table S1). Differences in survival between these two strains show that the ΔSOD nematodes actually exhibited increased radiation fitness and a longer life span compared to the WT growing under intense gamma radiation. The results of statistical analyses of the data used a parametric survival regression model based on the Weibull distribution (Table S2). This analysis implies that the absence of SOD (coded by the SOD variable) in fact significantly reduced the radiation death hazard (*P* value = 0.00101). We note that the ΔSOD worms had better radiation survival than the wild-type, yet the initial levels of H-Mn in the *C. elegans* strains were the same (Fig. 3A). While this may suggest that something other than H-Mn is responsible, the distribution of Mn antioxidants in *C. elegans* cells is expected to change with the loss of MnSOD enzymes in mitochondria (see Discussion).

***D. radiodurans* and *L. plantarum* become desiccation-sensitive upon loss of MnSOD.**

Both desiccation-induced hyperoxic conditions and ionizing radiation produce $O_2^{\bullet-}$, whose damage to cell functions can result in mutations and death. For example, the aerobic dehydration of *D. radiodurans* for 6 weeks causes approximately 60 DNA double-strand breaks (DSBs) per genome, the same as caused by exposure to 6 kGy of gamma rays (12). Although such findings appear to support the idea that the etiologic ROS underlying radiation and desiccation toxicity are the same, it is of significance that the primary location of $O_2^{\bullet-}$ generation in cells is different in the two cases. In drying cells, $O_2^{\bullet-}$ is the product of direct contact with atmospheric O_2 , and thus $O_2^{\bullet-}$ forms near the cell surface; in irradiated cells, $O_2^{\bullet-}$ is derived mostly from H_2O_2 produced by water radiolysis and is formed throughout the

FIG 3 Legend (Continued)

blotting carbonyl analysis (Oxyblot), which reveals the presence (black) or absence (no signal) of protein oxidation. CEU was compared to *D. radiodurans* ultrafiltrate (DRU) of WT (d2) bacteria. Noncontiguous portions of the same blot are separated by white lines. (G) CEU of WT (d2) nematodes preserves the activity of an irradiated enzyme. BamHI was irradiated in potassium phosphate buffer (PiB) or in CEU or DRU and then incubated with lambda phage DNA and subjected to agarose gel electrophoresis. Noncontiguous portions of the same agarose gel are separated by white lines.

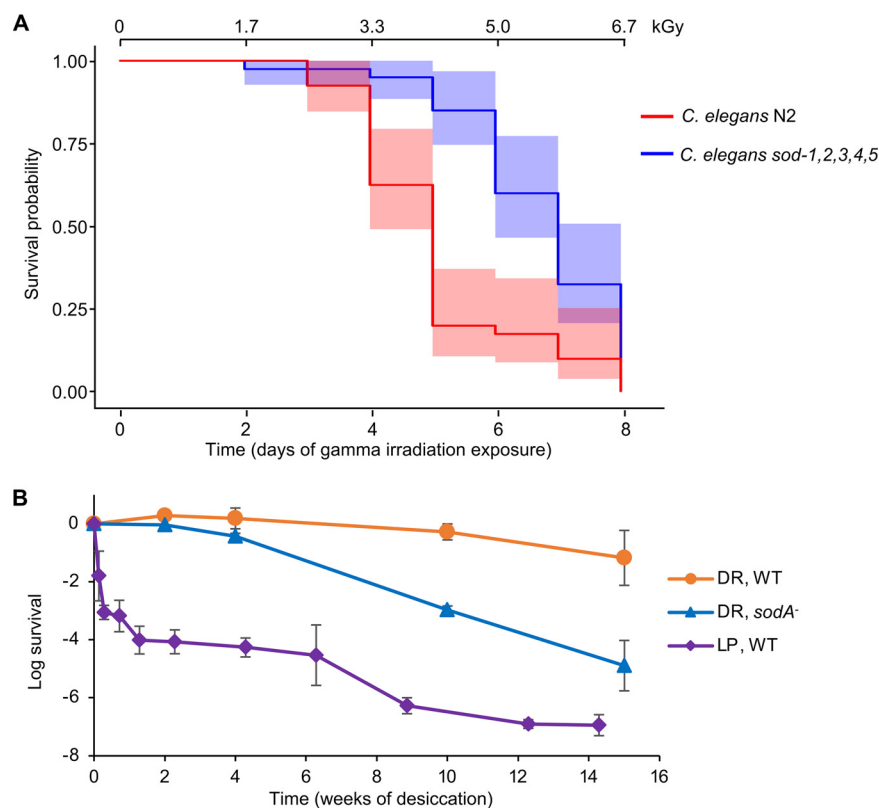


FIG 4 Differential effects of MnSOD on radiation and desiccation tolerance. (A) Comparison of Kaplan-Meier survival curves for irradiated WT (N2) (red) and Δ SOD (*sod-1,2,3,4,5*) (blue) *C. elegans* strains. Ten gravid adult worms per group were inoculated on plates (NGP) with OP50 lawns (4 plates/group) and monitored for survival and scored for activity over 8 days under 34.75 Gy/h (^{137}Cs). Shaded regions represent 95% Cis; the *P* value based on regression analysis described in the main text was 0.00101. This result was similar in two independent experiments. (B) Desiccation resistance of WT and Δ MnSOD *D. radiodurans* and WT *L. plantarum*. Cells were grown to the early stationary phase, desiccated at room temperature in a hermetically sealed chamber containing Drierite (CaSO_4), and tested for viability by CFU analysis after the indicated number of weeks. CFU time points were in triplicate; standard deviations are shown.

cell (26). We thus tested whether MnSOD, which is dispensable in *D. radiodurans* resistance to radiation-induced ROS, also is dispensable for resistance to desiccation, which is a more commonly encountered environmental oxidative stressor. We further complemented this by examining the desiccation resistance of *L. plantarum*, a radiation-resistant bacterium (4, 47) (Fig. S4) that also accumulates Mn antioxidants but does not encode enzymatic SODs (4, 37, 38).

We report the first demonstration that the *sodA*⁻ *D. radiodurans* mutant is rendered desiccation-sensitive. Fig. 4B shows the desiccation survival curves for WT and *sodA*⁻ *D. radiodurans* over 15 weeks under ambient atmospheric conditions. The *sodA*⁻ mutant is in fact far more sensitive to desiccation than the WT; it survived 1,000 \times less well after desiccation for 10 weeks. Correspondingly, *L. plantarum*, which is devoid of SODs, is even more desiccation-sensitive (Fig. 4B). Thus, Mn antioxidants do not substitute for MnSOD in slowly desiccating bacterial cells under atmospheric conditions, namely, 21% O_2 .

Finally, we confirmed by phenotypic analyses that the *sodA*⁻ *D. radiodurans* mutant remains resistant to chronic gamma irradiation and ultraviolet C (UVC) irradiation (Fig. 5A and B). However, the mutant is rendered hypersensitive to paraquat (methyl viologen) (Fig. 5C), a powerful redox-active $\text{O}_2^{\bullet-}$ -generating herbicide (52).

DISCUSSION

The spectroscopic measure of cellular Mn antioxidant (H-Mn) content is currently the strongest known biological indicator of cellular radiation resistance (5). This remarkable association was first demonstrated in archaea, bacteria, and yeasts grown to the early stationary

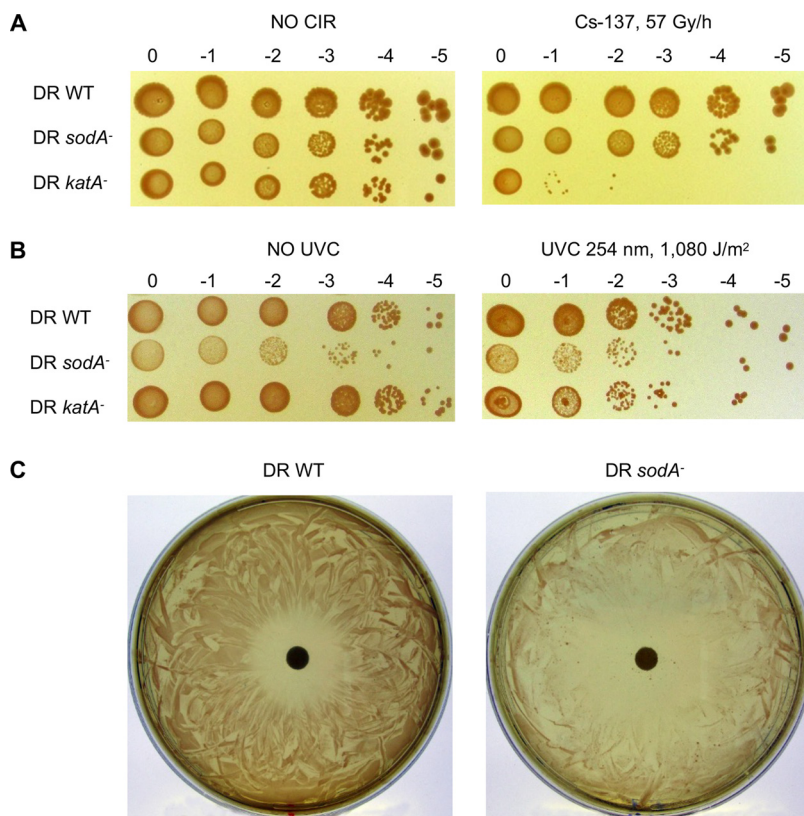


FIG 5 Oxidative stress resistance phenotypes of *D. radiodurans* (DR) WT, *sodA*⁻, and *katA*⁻ (catalase-deficient) under aerobic growth conditions. (A) Chronic gamma irradiation (CIR) (¹³⁷Cs). Proliferation of bacteria under 57 Gy/h for 6 days. In this panel, the dilutions shown are on a log₁₀ scale and represent order of magnitude changes in initial cell concentration. (B) UVC irradiation (254 nm). Clonogenic survival after an acute UVC dose of 1 kJ/m². Dilutions are as in panel A. (C) Paraquat. Hypersensitivity of *sodA*⁻ colony biofilm growth to paraquat applied to the central disc, which contained 20 µL 12.5 mM methyl viologen dichloride.

phase when cells are the most resistant (5). However, it was unknown whether or not the H-Mn content of a given organism is fixed or varies over its life span; neither was it known if EPR is sufficiently sensitive to detect life stage-dependent changes in radioresistance. We experimentally manipulated the cellular H-Mn content of cells by aging; EPR spectra collected over a 10-day aging study of *D. radiodurans* correspondingly show progressive loss of H-Mn antioxidants as the medium becomes depleted (Fig. 2C and D), as is quantified in Fig. 2E, and this tracks with the loss in radiation resistance (Fig. 2A and B). This result is similar to H-Mn responses observed over the life span of *C. elegans* nematodes (Fig. 3).

As small-molecule H-Mn antioxidants globally protect the proteome of cells (20, 21), this most likely includes protection of MnSOD; the radiation-stable H-Mn “defender” protects the radiation-sensitive one (26). The correlation of age with decrease in H-Mn content might be thought to suggest that as the cells age and the pool of metabolites that bind to Mn²⁺ to form H-Mn antioxidants gets consumed, the cells eventually rely solely on enzymatic SOD defenses. This view would then predict that old cells of Δ MnSOD *D. radiodurans* and *C. elegans* are more radiation-sensitive than WT. However, our results contradict this idea and even appear to pose a further puzzle; we find that the Δ MnSOD *D. radiodurans* mutant lacking any SOD activity (52) consistently displayed not merely undiminished, but indeed modestly increased radiation fitness (Fig. 2A and B; see also Fig. S1D and E). *Caenorhabditis elegans*, known to be highly radiation-resistant, had been viewed as presenting this same puzzle, in that mutants devoid of SODs have undiminished life spans compared to WT and, as we now show, even under intense gamma irradiation (Fig. 4A).

In discussing the correlation of MnSOD and Mn antioxidant content to aging and oxidative stress resistances, we integrate them with those of previous studies, which leads

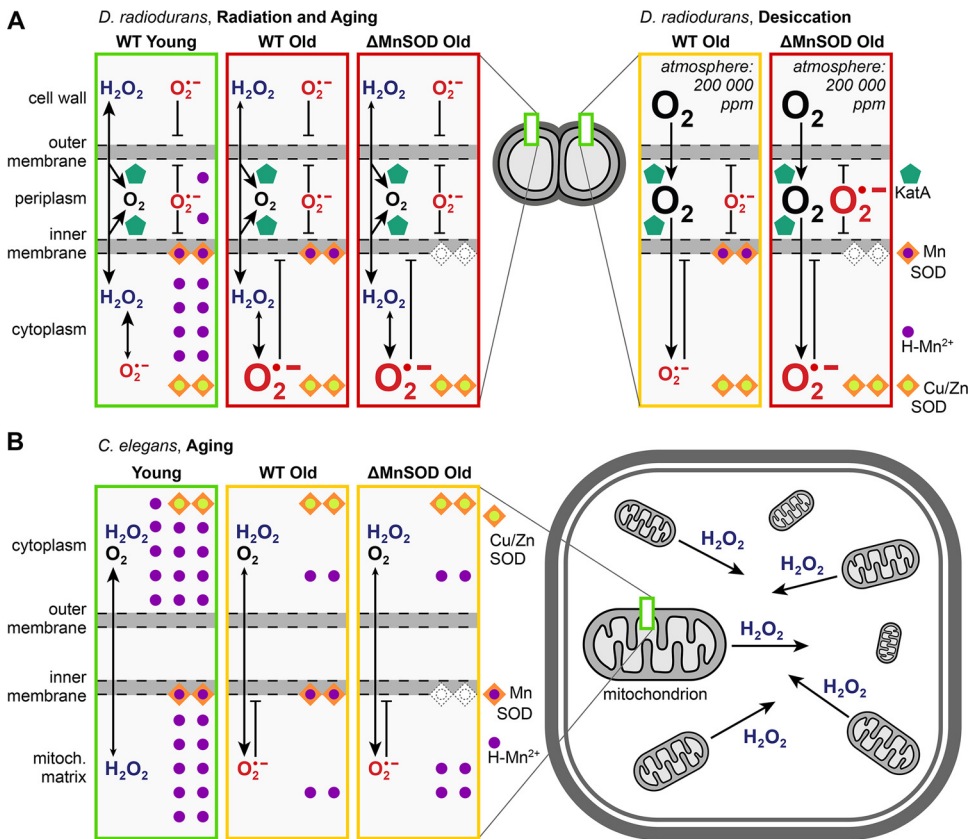


FIG 6 Role of H-Mn antioxidants and MnSOD enzymes in radiation- and desiccation-resistant organisms. (A) *D. radiodurans*; radiation and aging (left) (Fig. 5A). In irradiated cells, $\text{O}_2^{\bullet-}$ is derived mostly from H_2O_2 produced by water radiolysis and is formed throughout the cytoplasm. $\text{O}_2^{\bullet-}$ is membrane impermeable and becomes trapped in cells. Desiccation (right) (Fig. 4B). During desiccation, $\text{O}_2^{\bullet-}$ is the product of metabolism in cells in direct contact with atmospheric O_2 , and thus $\text{O}_2^{\bullet-}$ forms near the cell surface. H-Mn antioxidants accumulate in young cells and catalyze the same $\text{O}_2^{\bullet-}$ dismutation reaction as MnSOD, yielding H_2O_2 . Catalase (KatA) is periplasmic. (B) *C. elegans*; aging (Fig. 3B to D and Fig. 4A). The essential $\text{O}_2^{\bullet-}$ -scavenging features of H-Mn antioxidants and MnSOD in mitochondria are the same as for *D. radiodurans*, except that mitochondria release H_2O_2 into the cytoplasm; MnSOD is resident in the matrix and therefore distal to cell surfaces most exposed to O_2 , and loss of MnSOD adds Mn^{2+} ions to the pool of Mn antioxidants in the matrix.

us to a broadened picture of cellular defense against oxidative stress. EPR spectroscopy has resolved the apparent puzzle presented by these two organisms by showing that this MnSOD-independent resistance in both is associated with the hyperaccumulation of radio-protective H-Mn (Fig. 2C and D; Fig. 3C and D), as confirmed analytically (Fig. 3F and G). Our data thus show that radiation fitness and life span can be decoupled from enzymatic-MnSOD defenses in *D. radiodurans* and *C. elegans*; our findings imply that H-Mn antioxidants supplant at least some enzymatic SOD functions in *Deinococcus* bacteria as well as in *C. elegans* mitochondria, as visualized in the scheme of Fig. 6.

Of course, the enzyme MnSOD does play a critical role in $\text{O}_2^{\bullet-}$ scavenging and resistance to extreme oxidative stress other than radiation insult in these two organisms. For example, MnSOD deletion mutants render *D. radiodurans* and *C. elegans* hypersensitive to paraquat (43, 46, 52–54) (Fig. 5C), and we show here that ΔMnSOD *D. radiodurans* is desiccation-sensitive (Fig. 4B). This hitherto unknown contrast between the importance of MnSOD in protection against the hyperoxic conditions of desiccation (and paraquat), and yet the absence of deleterious effects on radiation resistance and aging from the elimination of MnSOD in ΔMnSOD mutants, implies that Mn antioxidants and SOD enzymes serve different roles in antioxidant defense (Fig. 6A).

This conclusion is reinforced by considering the bacterium *L. plantarum*, which is unusual in that it does not encode enzymatic $\text{O}_2^{\bullet-}$ scavengers, but hyperaccumulates Mn antioxidants (Fig. 3A) and, as a result, is radiation-resistant (4, 5, 13, 37, 38, 47) (Fig. 54). And

again, with *L. plantarum*, as with *D. radiodurans*, the absence of an enzymatic $O_2^{\bullet-}$ defense accompanies sensitivity to desiccation (Fig. 4B). The need for MnSOD during desiccation of both bacteria studied here suggests a fundamental role of this enzyme is to defend nutrient-restricted or starving cells that are directly exposed to the high atmospheric levels of O_2 , a common combination (12, 44) (Fig. 6A). The distribution of SOD enzymes in a cell also shapes our considerations. For example, MnSOD is resident in the cytoplasm and associated with membranes of *Deinococcus* cells (55, 56), whereas in *C. elegans* cells, MnSOD is localized within the mitochondrial matrix; it is Cu/ZnSOD that is resident in the cytoplasm and implicated in desiccation-survival of dauer larvae, a developmentally arrested form induced by starvation (57–60).

An extended theory of oxidative stress. The observation that Δ MnSOD strains of *D. radiodurans* and *C. elegans* show both an undiminished life span and undiminished radiation resistance contradicts the current oxidative damage theory, which identifies MnSOD as the preeminent defense against the $O_2^{\bullet-}$ generated during irradiation as well as aging. Our results show that this paradox is removed if the defense against oxidative stress is extended to include H-Mn as complementary to MnSOD (Text S2).

The extended oxidative stress theory clearly explains the absence of deleterious effects on *D. radiodurans* radiation resistance caused by the absence of MnSOD in young and mature Δ MnSOD cells. We attribute the puzzling modest increase in life span and radiation survival of aging Δ MnSOD bacteria to the lag in growth (Fig. 2F). This growth delay would certainly conserve nutrients that facilitate radiation survival and longevity (40). For *C. elegans*, mutants lacking SODs also have undiminished life spans compared to those of the WT (42, 43), even under intense gamma irradiation (Fig. 4A). Once again, this can be explained through protection by Mn antioxidants. We note that mitochondria are reported to accumulate 10 to 20 mmol/L Mn^{2+} , which is 10 to 20 times more Mn than accumulated overall in *D. radiodurans* and in the range of Mn concentrations in *L. plantarum* (20, 37, 38, 61, 62). In both *L. plantarum* and *C. elegans*, EPR shows that, essentially, all this Mn^{2+} is present in the radioprotective H-Mn form (Fig. 3A), which shows that both cytosolic Mn^{2+} and Mn^{2+} in mitochondria in fact all exist as H-Mn, explaining the similar responses of the nematodes and the bacteria (Fig. 6). In *L. plantarum* bacteria, the accumulated Mn^{2+} antioxidants (H-Mn) bind carboxylic acids (e.g., lactate) to form Mn antioxidants (27) (Fig. 3A).

Our finding that Mn antioxidants hyperaccumulated in *C. elegans* are exceptionally protective of proteins (Fig. 3F and G) and that H-Mn content drops precipitously in the last third of the life span (Fig. 3E) together explain reports that the steady-state level of oxidized proteins increases exponentially during the last third of the life span in animals (31). However, a more detailed understanding of why the loss of MnSOD in *C. elegans* actually appears to facilitate survival under intense irradiation (Fig. 4A) would benefit from a determination of the metrics of Mn distribution and the composition of the pool of Mn^{2+} -binding metabolites in its mitochondria. In our model, MnSOD competes with metabolites for Mn^{2+} , and the loss of Mn-enzymes increases the cellular budget of free Mn^{2+} , which leads to enhanced radiation survival in the worms (Fig. 6B, Δ MnSOD). The model may even explain reports by others that the presence of MnSOD can actually amplify radiosensitivity in bacteria (63). However, until there is a genetic route to control Mn antioxidant content, we cannot rule out the possibility that an as yet unidentified factor may be the causal agent governing age-dependent decreases in radiation resistance.

If H-Mn is indeed complementing MnSOD, as proposed here, then Mn^{2+} ion supplementation alone should facilitate oxidative survival, and this in fact has been observed in several studies; Mn^{2+} added to *D. radiodurans* and *E. coli* facilitates radiation survival (4, 13, 15), and Mn^{2+} addition to a short-lived, paraquat-sensitive *C. elegans* mutant (*mev-1*) accelerates development, enhances stress resistance, and rescues the life span (64). Likewise, supplementation of mice with $MnCl_2$ alone markedly increases ionizing radiation survival (65). Collectively, these observations can now be understood as resulting from the increased amounts of cellular Mn^{2+} in the form of radioprotective H-Mn complexes (Fig. 6A and B).

To summarize, the present results for WT and Δ MnSOD of *D. radiodurans* and *C. elegans*, and for the radioresistant *L. plantarum*, which does not express SODs, show that

radioresistance is not supported by MnSOD. This suggests that Mn antioxidants have comparable or greater efficacy in this role, with wider cellular distribution than MnSOD. Finally, that H-Mn cannot protect cells from atmospheric O₂ during desiccation (Fig. 4B) is implicit in the nature of this stress; starving cells cannot accumulate the metabolites that coordinate to Mn²⁺ to form Mn antioxidants, which leaves MnSOD as the only defense against elevated O₂^{•−} in cells that are hyperoxic because they are exposed directly to the atmosphere (Fig. 6A). The extended oxidative stress defense theory further explains the radiosensitivity of the *E. coli* K-12 and *S. cerevisiae* EXF-6218 (5) (Fig. 3A). In those cells, radioprotective H-Mn is only a small minority of the nonenzymatic Mn²⁺ and thus can do little to defend against a sudden buildup of cytoplasmic O₂^{•−}, whereas in *D. radiodurans* cells, antioxidant H-Mn is the major form of Mn²⁺ and thus the major defense against radiation.

Looking forward, EPR spectroscopic methods now offer a novel path to bridging the gap between *in vitro* and *in vivo* approaches to further testing and, as needed, further improving the modified oxidative stress defense mechanism. One might further consider an even more dramatic possible application for the use of EPR to monitor Mn²⁺ speciation *in vivo*. Viewing *C. elegans* nematodes (Fig. 3) as surrogates for human tissues, the present results suggest a possible use of EPR to examine cancer biopsies samples. An EPR determination of the amount of antioxidant Mn in a biopsy sample, and thus the radiation resistance of an individual tumor, might well assist in optimizing a radiation/chemotherapeutic regime for specifically attacking that tumor (66).

Conclusions. We experimentally manipulated the cellular H-Mn antioxidant content by aging viable cultures of *D. radiodurans* (Fig. 2A to E) and *C. elegans* (Fig. 3 and 4A), and showed that MnSOD is expendable for the radiation survivability and longevity of the organisms. However, the well established role of MnSOD in defense against oxidative stress is nonetheless exemplified by the fact that its absence makes the *D. radiodurans* ΔMnSOD mutant sensitive to the exposure to atmospheric O₂ attendant to desiccation and to the O₂^{•−}-generating paraquat, as well as delaying growth compared to the WT (Fig. 2F, 4B, and 5C). These complementary roles of H-Mn antioxidants and MnSOD against various forms of oxidative stress are also displayed by *L. plantarum*, which does not encode SODs but hyperaccumulates H-Mn antioxidants and thus is strongly radiation-resistant but sensitive to desiccation (Fig. 4B; see also Fig. 54). Such findings require extension of Denham Harman's theory to include accumulated H-Mn antioxidants as partners and complements to MnSOD (1, 2, 5).

The extended theory of oxidative stress defense posits that MnSOD and H-Mn antioxidants play complementary roles in defense against oxidative stress caused by O₂^{•−}. This formulation solves the apparent puzzle presented by observations in model organisms that radiation resistance and longevity are independent of MnSOD, while defense against other modes of oxidative stress are not (3, 56, 67–69).

MATERIALS AND METHODS

Bacteria. The WT bacterial strains used were as follows: *Deinococcus radiodurans* (USUHS) (ATCC BAA-816), *Lactobacillus plantarum* (ATCC 14917), and *Escherichia coli* (strain K-12 MG1655). The ΔMnSOD *D. radiodurans* MD885 is isogenic with ATCC BAA-816 and was derived by transfer of the disrupted *sodA* locus (DR1279) of KKW7003 by kanamycin selection (52); the catalase A (*katA*[−]) mutant is KKW7003 (52); *E. coli* mutant strain OP50 is a uracil auxotroph; OP50-1 is also streptomycin-resistant.

Yeasts. The WT *Saccharomyces cerevisiae* strain EXF-6218 was chosen from a collection of fungi previously gauged for gamma radiation resistance. Strain EXF-6218 is a diploid and one of the most radiation-sensitive *S. cerevisiae* strains reported (5, 35).

Nematodes. The WT *Caenorhabditis elegans* strain N2 was originally obtained from David Eisenmann, University of Maryland Baltimore County and was used as a control strain in the nematode studies. The following ΔSOD mutant strains were compared to N2: MQ1766 is a quintuple *sod-1,2,3,4,5* [*sod2(ok1030)* I; *sod5(tm1146)* *sod1(tm783)* II; *sod4(gk101)* III; *sod3(tm760)* X] mutant with complete loss of MnSOD and Cu/ZnSOD activities; GA480 is a *sod-2,3* [*sod2(gk257)* I; *sod3(tm760)* X] double mutant deficient in MnSOD enzymes (ΔMnSOD); GA184 *sod-2* [*sod2(gk257)* II], RB1072 *sod-2* [*sod2(ok1030)* II], and GA186 *sod-3* [*sod-3(tm760)* X] are single ΔMnSOD mutants. All mutants were purchased from Caenorhabditis Genetics Center (CGC), University of Minnesota.

***D. radiodurans* growth, gamma irradiation, and samples for EPR.** WT *D. radiodurans* (ATCC BAA-816) was inoculated into defined liquid TGY rich medium (1% bacto-tryptone, 0.5% yeast extract, and 0.1% glucose). ΔMnSOD *D. radiodurans* (MD885) was inoculated into TGY supplemented with 25 μg/mL kanamycin (TGY-Km25). Both cultures were incubated with orbital shaking at 200 rpm at 32°C up to an optical density at 600 nm (OD₆₀₀) of ~0.9, which corresponds to the mid-exponential phase of growth. Mid-exponential-phase WT and *sodA*[−] *D. radiodurans* cells were then inoculated into two 2-L flasks with

0.8 L TGY or TGY-Km25. This corresponded to an inoculation of approximately 10^5 CFU/mL, followed by incubation with aeration (200 rpm orbital shaking) at 32°C for 10 days without change of broth.

Mid-exponential-phase (young) actively dividing cells were harvested when a culture reached OD₆₀₀ 0.9, defined as day 1 (d1). After an additional 24 h (d2), early-stationary-phase (mature), metabolically active but nondividing cells were harvested from liquid medium; late-stationary-phase (old) cells were harvested at 144 h (d6), and mostly replication-defective cells on d10. The *D. radiodurans* WT and Δ MnSOD cells thus isolated at each stage were irradiated acutely at 8.8 kGy/h (⁶⁰Co) on ice, and age-dependent survival was determined by CFU assay after exposure to 0, 10, and 15 kGy (⁶⁰Co) (70, 71). Samples were serially diluted using TGY medium, and the dilutions were plated on TGY agar plates (100 μ L per plate). CFU were counted after 1 week at 32°C (Fig. 2A, B, and F; see also Fig. S1A).

For EPR analysis, 30-mL cultures (1×10^8 to 3×10^8 CFU/mL) were harvested by centrifugation, and cells were washed twice with MilliQ water from “Banstead Nano Pure Diamond” [Thermo Scientific] and resuspended in 0.3 mL 20% Glycerol (vol/vol) MilliQ water. EPR tubes (quartz, inner diameter 2.1 mm, length 65 to 70 mm; Wilmad-LabGlass) were filled with $\sim 80 \mu$ L of the concentrated cell suspensions and stored frozen at -80°C for EPR analyses.

Establishment and maintenance of *C. elegans* colonies on NGM agar plates. Colonies of the following *C. elegans* strains were established and maintained on nematode growth medium (NGM) agar and fed OP50 *E. coli*. Strain Bristol N2 (WT) (a gift from David Eisenmann, UMBC, Baltimore, MD) and SOD mutants (see above, “Nematodes”) were provided by the CGC, funded by the NIH Office of Research Infrastructure Programs (P40OD010440). Briefly, $\sim 1,000$ worms were maintained at ambient temperature on a 100-mm petri dish containing NGM medium (1.7% agar [wt/vol], 50 mM NaCl, 0.25% peptone [wt/vol], 1 mM CaCl₂, 5 μ g/mL cholesterol, 25 mM KH₂PO₄, and 1 mM MgSO₄) and seeded with a lawn of *E. coli* OP50 as the food source. As the OP50 lawns were depleted, an $\sim 1\text{-cm}^2$ section of agar (containing worms) was incised from the agar plate and inverted onto a fresh lawn of OP50, thus giving the worms sufficient nutrients to continue developing and reproducing.

Establishment and maintenance of *C. elegans* culture in axenic medium. *C. elegans* cultured on NGM medium with OP50 was allowed to reach a density of $\sim 85\%$ gravid adult worms (3 to 5 days). They were rinsed from the plate in sterile distilled water (dH₂O), and pelleted at $10,000 \times g$ for 30 s; the supernatant was discarded. The worms were repeatedly rinsed and pelleted as above. *C. elegans* eggs were isolated from the gravid adults by incubating the worm pellet in freshly prepared 20% alkaline hypochlorite solution (0.25 M NaOH, 20% bleach) for 3 to 5 min with occasional vortexing. The suspension was monitored for dissociation of adult worms and egg release. The eggs were pelleted ($10,000 \times g$ for 30 s), rinsed 3 times with sterile dH₂O, and resuspended in 3 mL of fresh sterile dH₂O. The egg suspension was transferred to a clean 15-mL conical tube and incubated overnight at ambient temperature with gentle shaking, allowing for egg hatch and developmental arrest of larval stage 1 (L1) worms.

The newly hatched L1 larvae were pelleted ($800 \times g$ for 3 min), the supernatant was discarded, and the worms were resuspended in 10 mL of axenic medium. The suspension was transferred to a T25 polystyrene culture flask and incubated at ambient temperature with gentle shaking. Cultures were expanded to 30 mL of medium in T75 flasks and subcultured weekly to maintain a viable worm concentration of $\sim 20,000$ worms/mL. The axenic medium used in this study is a modified version of that previously described (72, 73). A $2\times$ stock of custom-ordered *C. elegans* maintenance medium (CeMM; MediaTech, Inc.) was diluted to a $1\times$ working stock and supplemented with 20 μ M hemin chloride, 10% ultrapasteurized (UHT) skim milk, 5 μ g/mL cholesterol, 100 μ g/mL tetracycline, and 100 units/mL of penicillin-streptomycin.

***C. elegans* sample preparation for EPR analysis.** The EPR study of *C. elegans* populations began by inoculating $\sim 3,000$ L1 worms (WT and *sod* mutants) into 30 mL of fresh axenic liquid medium (ALM), yielding an optimal density of 20,000 worms/mL in 4 to 5 days at ambient temperature (74). In that time, the worms grew from $\sim 200 \mu\text{m}$ in length into $\sim 1\text{-mm}$ adults. We collected EPR spectra for intact WT and Δ SOD worms over their life span. Under our growth conditions, *C. elegans* lived 18 to 26 days, displaying the following stages: young worms (d1 to d3), mature (middle-aged) worms (d5 to d13), old worms (d15 to d21), and unresponsive worms (d26 to d33). One milliliter of axenically cultured *C. elegans* was collected at the indicated times and harvested by centrifugation ($16,000 \times g$, 30 s). Worms were washed twice with 1 mL of MilliQ water, pelleted, and resuspended in 200 μ L 20% glycerol in MilliQ water (vol/vol). Two EPR tubes were filled with $\sim 80 \mu$ L of the worm suspension. All EPR samples were stored at -80°C and transferred to liquid nitrogen prior to their being shipped to Northwestern University for EPR analysis.

EPR spectroscopy. 35-GHz continuous-wave (CW) EPR spectra were recorded using a lab-built EPR spectrometer (75). Absorption-display EPR spectra of frozen cells were collected in the “rapid passage” mode at 2 K as previously described (5, 76) (experimental conditions: medium wave [MW] frequency, 34.9 GHz; MW power, 1 mW; temperature, 2 K; modulation amplitude, 2 G; time constant, 64 ms; scan rate, 1 kG/min). Data acquisition was done using a home-written program in LabVIEW. EPR spectra were simulated using the software EasySpin (5.2.30). For details of the procedures for determining the fractional contributions of H-Mn and L-Mn to the Mn²⁺ EPR spectra, see reference 5.

Chronic gamma irradiation of *C. elegans*. *C. elegans* strains Bristol N2 (WT) and MQ1766 (*sod-1,2,3,4,5*) were cultured on NGM plates seeded with OP50 bacteria and prepped as described above for egg isolation and L1 larvae synchronization (see above, “Establishment and Maintenance of *C. elegans* Culture in Axenic Medium”). The newly hatched L1 larvae were resuspended in 200 μ L dH₂O, transferred to fresh NGM plates seeded with OP50 bacteria (NGM/OP50 plates), and maintained at ambient temperature until they reached the young adult stage (N2, ~ 4 days of incubation; Δ SOD mutants ~ 6 days of incubation). Then, 80 young adult worms of each strain were transferred to fresh 60-mm NGM/OP50 plates at 10 worms per plate.

Four plates of each strain were exposed to the ¹³⁷Cs source, which generated a dose rate of 34.74 Gy/h and a temperature range of 23 to 26°C, for 8 days. Four control plates per strain were maintained for 8 days in

the dark at a comparable temperature. Worms were monitored daily for mobility and developmental progression.

***C. elegans* and *D. radiodurans* protein-free small-molecule cell extract (ultrafiltrate) preparation.** *C. elegans* WT strain Bristol N2 was grown on NGM/OP50-1 plates for egg isolation and L1 larvae synchronization as described above. Synchronized day 2 L4-stage worms were washed with M9 minimal medium (6 mg/mL of K_2HPO_4 and 3 mg/mL of KH_2PO_4 , 1 mg/mL of NH_4Cl , and 0.5 g of NaCl, 1 mM $MgSO_4$) off the NGM plates and agitated on a rocker for 1 h to allow full digestion of OP50-1 *E. coli* in worm intestines. The worm sample was washed in a cycle of additions of M9 and removal of M9 after centrifugation at $2,000 \times g$ for 1 min each, with the final washing in 50 mM phosphate buffer, pH 7.4, and concentrated by centrifugation at $2,000 \times g$ for 1 min. Supernatant was removed and worms were resuspended in lysis buffer (50 mM phosphate buffer, pH 7.4, 10 mM KCl, 1.5 mM $MgCl_2$, 1 mM DTT, and $2 \times$ EDTA-free protease inhibitor cocktail), twice the volume of the worm pellet based on Stiernagle 2006. The worms were then lysed using sonication and multiple freeze-thaw cycles in liquid nitrogen and spun at $1,000 \times g$ for 10 min to remove nuclei and worm debris. The supernatants of the worms from the $1,000 \times g$ spin were then centrifuged at $20,000 \times g$ for 30 min to generate the soluble fraction. The soluble protein concentration was determined using protein assay kit (Bio-Rad), and the supernatant was adjusted to 20 mg/mL protein by dilution with MilliQ water. The supernatants were then ultracentrifuged at $190,000 \times g$ (69 h, $4^\circ C$), and the ultracentrifuged supernatants were subjected to filtration through 3-kDa Centrplus centrifugal filter devices (YM-3) (Millipore Corporation, Bedford, MA, USA) at room temperature for 3 to 4 h. The ultrafiltrates were then concentrated $5 \times$ in a SpeedVac concentrator (Savant, GMI, Inc., Ramsey, MN, USA) at room temperature, boiled for 30 min, aliquoted, and stored at $-80^\circ C$. *D. radiodurans* ultrafiltrate was prepared similarly (5, 15). Briefly, *D. radiodurans* cells were grown as a batch culture (in 1.5 L TGY medium) to an optical density of 0.9 (mid-exponential phase) determined at 600 nm. Harvested cells were washed twice in MilliQ water, centrifuged at $3,000 \times g$ for 15 min at $4^\circ C$, and broken open in MilliQ water by passage through a One-Shot cell disrupter (38,000 lb/in 2). Upon lysis, the crude *D. radiodurans* cell extract was centrifuged at $12,000 \times g$ (1 h, $4^\circ C$), yielding an aqueous phase which contained water-soluble proteins and small molecules and a pellet of insoluble cell debris (15). The soluble protein concentration was determined, followed by ultracentrifugation and ultrafiltration. The ultrafiltrate was then concentrated 5 times at room temperature, boiled for 30 min, aliquoted, and stored at $-80^\circ C$.

Pre- and postirradiation protein carbonylation detection. Protein carbonylation was detected as described previously (15) with small modifications. Soluble protein fractions purified from an *E. coli* (K-12 MG1655) homogenate were used as the substrate for carbonyl analyses. Proteins were prepared from *E. coli* grown in TGY to OD $_{600}$ 0.9. Cells were broken open by passage through a One-Shot cell disrupter (38,000 lb/in 2). Insoluble proteins and cell debris were removed by centrifugation at $31,000 \times g$ (1 h, $4^\circ C$). The supernatant containing soluble *E. coli* proteins was subjected to ultracentrifugation ($190,000 \times g$ [69 h, $4^\circ C$]), and the protein pellet was dissolved in MilliQ water and quantified for concentration using the protein assay kit (Bio-Rad). The proteins were stored at $-80^\circ C$ as 44-mg/mL stocks in 150- μ L aliquots, which were used once and then discarded. Before irradiation, a stock of *E. coli* proteins was diluted in MilliQ H $_2$ O and concentrated *D. radiodurans* (DR) or *C. elegans* (CE) ultrafiltrate preparations, yielding mixtures with 4.4 mg/mL of *E. coli* protein in ultrafiltrate (50%). For a given *E. coli* protein-ultrafiltrate sample (44 μ L), ^{60}Co irradiations were kept on ice under aerobic conditions. At the indicated gamma radiation doses, 10- μ L samples were removed and stored on ice until the time course of irradiation was completed. The carbonyl groups in the *E. coli* protein samples were identified by the OxyBlot protein oxidation detection kit (Millipore, Sigma). Then, 10 μ g of *E. coli* protein after DNPH (2,4-dinitrophenylhydrazine) reaction neutralization was loaded on denatured polyacrylamide protein gel for carbonyl Western blotting.

Pre- and postirradiation activity of BamHI. Pre- and postirradiation activity of BamHI was determined as described previously (15, 20) with some modifications. BamHI (5,000 U/ μ L) (without bovine serum albumin [BSA]) (New England Biolabs, Ipswich, MA, USA) was diluted in *D. radiodurans* or in *C. elegans* ultrafiltrate to 0.54 U/ μ L. Then, 200 μ L of the BamHI mixture was gamma-irradiated aerobically on ice. Following irradiation, 20 μ L of each radiation-treated BamHI sample was assayed for residual endonuclease activity in separate reaction mixtures (final volume, 30 μ L) containing 125 ng lambda phage DNA, 50 mM NaCl, 10 mM Tris-HCl (pH 7.9), 10 mM $MgCl_2$, and 1 mM dithiothreitol (New England Biolabs; buffer 3). BamHI/lambda DNA mixtures were incubated for 1.25 h at $37^\circ C$, followed by agarose (0.8%) gel electrophoresis.

Gamma-irradiations of protein samples. *E. coli* soluble proteins mixed with ultrafiltrate samples and BamHI-ultrafiltrate samples were irradiated in 0.5-mL Eppendorf tubes on wet ice with ^{60}Co .

Growth of *D. radiodurans* under high-level chronic gamma irradiation (^{137}Cs). To evaluate the growth of *D. radiodurans* WT, *sodA* $^-$ (MD885), and *katA* $^-$ (KKW7003) strains under continuous gamma irradiation, cells were pregrown to an OD $_{600}$ of 0.9 ($\sim 10^8$ CFU/mL) in liquid TGY medium at $32^\circ C$ with shaking at 200 rpm. Cells were serially diluted (10^{-1} to 10^{-5}) in liquid TGY, and 5 μ L of each culture was spotted onto two separate TGY plates. All plates were incubated at 28 to $30^\circ C$ and sealed with Parafilm "M" laboratory film, one set exposed to 57 Gy/h within a ^{137}Cs irradiator and one set in the absence of radiation (outside the irradiator). The images were taken after 6 days of incubation under 57 Gy/h.

UVC irradiation. WT, *sodA* $^-$ (MD885), and *katA* $^-$ (KKW7003) *D. radiodurans* were grown in TGY or TGY-Km25 medium to the early stationary phase. Cells were serially diluted (10^{-1} to 10^{-5}) in liquid TGY, and 5 μ L of each culture was spotted onto two separate TGY plates. Opened petri plates were exposed to UVC (254 nm) for 18 min. Irradiance on plate surfaces was 1 W/m 2 , which gives radiant exposure of 1 J/m 2 /sec. The radiant exposure accumulated in 18 min was 1,080 J/m 2 .

Desiccation. WT and *sodA* $^-$ *D. radiodurans* cells were grown in TGY or TGY-Km25 medium to the early stationary phase (1×10^8 CFU/mL), transferred to Costar Stripwell 96-well microplates (Corning; catalog no. 9102), 25 μ L per well. The microplates were transferred to desiccation chambers with Drierite and stored at room temperature. For survival monitoring, the well contents were resuspended in 250 μ L of medium (dilution

factor of 10^{-1}), and the samples were diluted serially using TGY medium. The dilutions were plated on TGY agar plates (100 μ L of sample per plate). The plates were then incubated at 32°C for up to 1 week. For *L. plan-tarum*, desiccation survival assays were on cells in MRS medium at 37°C for 18 h.

Paraquat. Overnight cultures of *D. radiodurans* WT (in TGY medium) and *sodA*⁻ mutant MD885 (in TGY-Km25) in the volume of 100 μ L were spread as colony biofilms (lawns). Sterile paper disks saturated with 20 μ L of 12.5 mM paraquat (methyl viologen) dissolved in MilliQ H₂O were then placed on the middle of the plates, followed by incubation at 32°C for 6 days.

Statistics. For Fig. 4A, the data were compiled on irradiated WT (SOD⁺) (N2 strain) and Δ SOD (*sod-1,2,3,4,5*) (MQ1766 strain) *C. elegans* with survival as a function of time under chronic gamma irradiation at 34.74 Gy/h. All worms that became static (immobile) or were lost to observation were considered dead, and those that retained some mobility or twitching were considered alive. Based on these assumptions, survival analysis for WT and SOD⁻ worms was performed using the survival, survminer, and ggplot2 packages in R 4.0.3 software.

Kaplan-Meier survival curves were constructed with 95% confidence intervals (95% CIs) for each worm group. The curves could not be reliably compared by log rank test because the survival curves visibly crossed. For the same reason, proportional hazard modeling (Cox regression) was also unreliable because the Chi² test for the validity of the proportional hazard assumption (using the cox.zph command in R) returned a small *P* value of 0.00019.

To address these issues, a more flexible parametric survival modeling approach (mixed effect excess hazard models) using the mexhaz R package was implemented. In this method, the death hazard function was modeled using the Weibull distribution with one of the two parameters allowed to differ between the SOD⁺ and SOD⁻ worm groups. This approach could handle the situation where Kaplan-Meier survival curves for different groups crossed each other and the hazard functions were not proportional.

SUPPLEMENTAL MATERIAL

Supplemental material is available online only.

TEXT S1, DOCX file, 0.02 MB.

TEXT S2, DOCX file, 0.01 MB.

FIG S1, DOCX file, 0.3 MB.

FIG S2, DOCX file, 0.3 MB.

FIG S3, DOCX file, 0.3 MB.

FIG S4, DOCX file, 0.1 MB.

TABLE S1, DOCX file, 0.01 MB.

TABLE S2, DOCX file, 0.01 MB.

ACKNOWLEDGMENTS

We thank Brian Champine and Michael Woolbert (USUHS) for assistance in irradiator maintenance and calibration. We also thank Sofia C. Echelmeyer for graphical help.

This study was supported by NIH grant GM111097 (to B.M.H.) and by funds received from the Defense Threat Reduction Agency (DTRA) grant HDTRA1620354 (to M.J.D.) and from the USU Intramural Program to the Deinococcus Group. C.G. acknowledges the financial support from the state budget of the Slovenian Research Agency (grants J4-2549, P1-0198, and BI-US/18-20-032), and C.S. acknowledges the financial support from NIH grant 1 R15 GM090169-01. K.S.M.'s research is supported by the NIH Intramural Research Program at the National Library of Medicine. The funders had no role in study design, data collection and analysis, decision to publish, or preparation of the manuscript. The opinions expressed here are those of the authors and are not necessarily representative of those of the USUHS, HJF, DTRA, or NIH.

E.K.G., A.S., V.Y.M., B.J.-T., B.M.H., and M.J.D. designed the research; E.K.G., A.S., V.Y.M., B.J.-T., O.G., I.H.C., I.B., P.K., R.T., C.G., W.H.H., R.P.V., X.C., and C.S. performed the research; E.K.G., A.S., V.Y.M., K.S.M., B.J.-T., B.M.H., and M.J.D. analyzed the data; I.S. performed statistical analyses; and B.M.H. and M.J.D. wrote the manuscript.

We declare no competing interests.

The opinions expressed here are those of the authors and are not necessarily representative of those of the USUHS, Department of Defense (DoD), or the United States Army, Navy, or Air Force.

REFERENCES

1. Harman D. 1956. Aging: a theory based on free radical and radiation chemistry. *J Gerontol* 11:298–300. <https://doi.org/10.1093/geronj/11.3.298>.
2. Harman D. 1983. Free radical theory of aging: consequences of mitochondrial aging. *AGE* 6:86–94. <https://doi.org/10.1007/BF02432509>.

3. Shields HJ, Traa A, Van Raamsdonk JM. 2021. Beneficial and detrimental effects of reactive oxygen species on lifespan: a comprehensive review of comparative and experimental studies. *Front Cell Dev Biol* 9:628157. <https://doi.org/10.3389/fcell.2021.628157>.
4. Daly MJ, Gaidamakova EK, Matrosova VY, Vasilenko A, Zhai M, Venkateswaran A, Hess M, Omelchenko MV, Kostandarithes HM, Makarova KS, Wackett LP, Fredrickson JK, Ghosal D. 2004. Accumulation of Mn(II) in *Deinococcus radiodurans* facilitates gamma-radiation resistance. *Science* 306:1025–1028. <https://doi.org/10.1126/science.1103185>.
5. Sharma A, Gaidamakova EK, Grichenko O, Matrosova VY, Hoeke V, Klimenkova P, Conze IH, Volpe RP, Tkavc R, Gostiñar C, Gunde-Cimerman N, DiRuggiero J, Shuryak I, Ozarowski A, Hoffman BM, Daly MJ. 2017. Across the tree of life, radiation resistance is governed by antioxidant Mn²⁺, gauged by paramagnetic resonance. *Proc Natl Acad Sci U S A* 114:E9253–E9260. <https://doi.org/10.1073/pnas.1713608114>.
6. Brim H, McFarlan SC, Fredrickson JK, Minton KW, Zhai M, Wackett LP, Daly MJ. 2000. Engineering *Deinococcus radiodurans* for metal remediation in radioactive mixed waste environments. *Nat Biotechnol* 18:85–90. <https://doi.org/10.1038/71986>.
7. Shuryak I, Sachs RK, Brenner DJ. 2010. Cancer risks after radiation exposure in middle age. *J Natl Cancer Inst* 102:1628–1636. <https://doi.org/10.1093/jnci/djq346>.
8. Hernández L, Terradas M, Camps J, Martín M, Tusell L, Genescà A. 2015. Aging and radiation: bad companions. *Aging Cell* 14:153–161. <https://doi.org/10.1111/acer.12306>.
9. Tong J, Hei TK. 2020. Aging and age-related health effects of ionizing radiation. *Rad Med Prot* 1:15–23. <https://doi.org/10.1016/j.radmp.2020.01.005>.
10. Johnson TE, Hartman PS. 1988. Radiation effects on life span in *Caenorhabditis elegans*. *J Gerontol* 43:B137–B141. <https://doi.org/10.1093/geronj/43.5.b137>.
11. Gems D, Doonan R. 2009. Antioxidant defense and aging in *C. elegans*: is the oxidative damage theory of aging wrong? *Cell Cycle* 8:1681–1687. <https://doi.org/10.4161/cc.8.11.8595>.
12. Mattimore V, Battista JR. 1996. Radioresistance of *Deinococcus radiodurans*: functions necessary to survive ionizing radiation are also necessary to survive prolonged desiccation. *J Bacteriol* 178:633–637. <https://doi.org/10.1128/jb.178.3.633-637.1996>.
13. Culotta VC, Daly MJ. 2013. Manganese complexes: diverse metabolic routes to oxidative stress resistance in prokaryotes and yeast. *Antioxid Redox Signal* 19:933–944. <https://doi.org/10.1089/ars.2012.5093>.
14. Barnese K, Gralla EB, Cabelli DE, Valentine JS. 2008. Manganous phosphate acts as a superoxide dismutase. *J Am Chem Soc* 130:4604–4606. <https://doi.org/10.1021/ja710162n>.
15. Daly MJ, Gaidamakova EK, Matrosova VY, Kiang JG, Fukumoto R, Lee DY, Wehr NB, Viteri GA, Berlett BS, Levine RL. 2010. Small-molecule antioxidant proteome-shields in *Deinococcus radiodurans*. *PLoS One* 5:e12570. <https://doi.org/10.1371/journal.pone.0012570>.
16. Lingappa UF, Yeager CM, Sharma A, Lanza NL, Morales DP, Xie G, Atencio AD, Chadwick GL, Monteverde DR, Magyar JS, Webb SM, Valentine JS, Hoffman BM, Fischer WW. 2021. An ecophysiological explanation for manganese enrichment in rock varnish. *Proc Natl Acad Sci U S A* 118:e2025188118. <https://doi.org/10.1073/pnas.2025188118>.
17. Webb KM, DiRuggiero J. 2012. Role of Mn²⁺ and compatible solutes in the radiation resistance of thermophilic bacteria and archaea. *Archaea* 2012:845756. <https://doi.org/10.1155/2012/845756>.
18. Berlett BS, Levine RL. 2014. Designing antioxidant peptides. *Redox Rep* 19:80–86. <https://doi.org/10.1179/1351000213Y.0000000078>.
19. Dai S, Xie Z, Wang B, Yu N, Zhao J, Zhou Y, Hua Y, Tian B. 2021. Dynamic polyphosphate metabolism coordinating with manganese ions defends against oxidative stress in the extreme bacterium *Deinococcus radiodurans*. *Appl Environ Microbiol* 87:e02785-20. <https://doi.org/10.1128/AEM.02785-20>.
20. Daly MJ, Gaidamakova EK, Matrosova VY, Vasilenko A, Zhai M, Leapman RD, Lai B, Ravel B, Li SM, Kemner KM, Fredrickson JK. 2007. Protein oxidation implicated as the primary determinant of bacterial radioresistance. *PLoS Biol* 5:e92. <https://doi.org/10.1371/journal.pbio.0050092>.
21. Bruckbauer ST, Minkoff BB, Yu D, Cryns VL, Cox MM, Sussman MR. 2020. Ionizing Radiation-induced Proteomic Oxidation in *Escherichia coli*. *Mol Cell Proteomics* 19:1375–1395. <https://doi.org/10.1074/mcp.RA120.002092>.
22. Gaidamakova EK, Myles IA, McDaniel DP, Fowler CJ, Valdez PA, Naik S, Gayen M, Gupta P, Sharma A, Glass PJ, Maheshwari RK, Datta SK, Daly MJ. 2012. Preserving immunogenicity of lethally irradiated viral and bacterial vaccine epitopes using a radio-protective Mn²⁺-Peptide complex from *Deinococcus*. *Cell Host Microbe* 12:117–124. <https://doi.org/10.1016/j.chom.2012.05.011>.
23. Gayen M, Gupta P, Morazzani EM, Gaidamakova EK, Knollmann-Ritschel B, Daly MJ, Glass PJ, Maheshwari RK. 2017. *Deinococcus* Mn²⁺-peptide complex: a novel approach to alphavirus vaccine development. *Vaccine* 35:3672–3681. <https://doi.org/10.1016/j.vaccine.2017.05.016>.
24. Tobin GJ, Tobin JK, Gaidamakova EK, Wiggins TJ, Bushnell RV, Lee WM, Matrosova VY, Dollery SJ, Meeks HN, Kouliavskaia D, Chumakov K, Daly MJ. 2020. A novel gamma radiation-inactivated Sabin-based polio vaccine. *PLoS One* 15:e0228006. <https://doi.org/10.1371/journal.pone.0228006>.
25. Dollery SJ, Zurawski DV, Gaidamakova EK, Matrosova VY, Tobin JK, Wiggins TJ, Bushnell RV, MacLeod DA, Alameh YA, Abu-Taleb R, Escatte MG, Meeks HN, Daly MJ, Tobin GJ. 2021. Radiation-inactivated *Acinetobacter baumannii* vaccine candidates. *Vaccines (Basel)* 9:96. <https://doi.org/10.3390/vaccines9020096>.
26. Daly MJ. 2009. A new perspective on radiation resistance based on *Deinococcus radiodurans*. *Nat Rev Microbiol* 7:237–245. <https://doi.org/10.1038/nrmicro2073>.
27. Archibald FS, Fridovich I. 1982. The scavenging of superoxide radical by manganese complexes: in vitro. *Arch Biochem Biophys* 214:452–463. [https://doi.org/10.1016/0003-9861\(82\)90049-2](https://doi.org/10.1016/0003-9861(82)90049-2).
28. Fridovich I. 1998. Oxygen toxicity: a radical explanation. *J Exp Biol* 201:1203–1209. <https://doi.org/10.1242/jeb.201.8.1203>.
29. Imlay JA. 2013. The molecular mechanisms and physiological consequences of oxidative stress: lessons from a model bacterium. *Nat Rev Microbiol* 11:443–454. <https://doi.org/10.1038/nrmicro3032>.
30. Liochev SI, Fridovich I. 2005. Cross-compartment protection by SOD1. *Free Radic Biol Med* 38:146–147. <https://doi.org/10.1016/j.freeradbiomed.2004.10.017>.
31. Levine RL, Stadtman ER. 2001. Oxidative modification of proteins during aging. *Exp Gerontol* 36:1495–1502. [https://doi.org/10.1016/s0531-5565\(01\)00135-8](https://doi.org/10.1016/s0531-5565(01)00135-8).
32. Krisko A, Radman M. 2013. Phenotypic and genetic consequences of protein damage. *PLoS Genet* 9:e1003810. <https://doi.org/10.1371/journal.pgen.1003810>.
33. Hassan HM, Fridovich I. 1977. Physiological function of superoxide dismutase in glucose-limited chemostat cultures of *Escherichia coli*. *J Bacteriol* 130:805–811. <https://doi.org/10.1128/jb.130.2.805-811.1977>.
34. Bruckbauer ST, Minkoff BB, Sussman MR, Cox MM. 2021. Proteome damage inflicted by ionizing radiation: advancing a theme in the research of Miroslav Radman. *Cells* 10:954. <https://doi.org/10.3390/cells10040954>.
35. Shuryak I, Tkavc R, Matrosova VY, Volpe RP, Grichenko O, Klimenkova P, Conze IH, Balygina IA, Gaidamakova EK, Daly MJ. 2019. Chronic gamma radiation resistance in fungi correlates with resistance to chromium and elevated temperatures, but not with resistance to acute irradiation. *Sci Rep* 9:11361. <https://doi.org/10.1038/s41598-019-47007-9>.
36. McNaughton RL, Reddi AR, Clement MH, Sharma A, Barnese K, Rosenfeld L, Gralla EB, Valentine JS, Culotta VC, Hoffman BM. 2010. Probing in vivo Mn²⁺ speciation and oxidative stress resistance in yeast cells with electron-nuclear double resonance spectroscopy. *Proc Natl Acad Sci U S A* 107:15335–15339. <https://doi.org/10.1073/pnas.1009648107>.
37. Archibald FS, Fridovich I. 1981. Manganese, superoxide dismutase, and oxygen tolerance in some lactic acid bacteria. *J Bacteriol* 146:928–936. <https://doi.org/10.1128/jb.146.3.928-936.1981>.
38. Archibald FS, Fridovich I. 1981. Manganese and defenses against oxygen toxicity in *Lactobacillus plantarum*. *J Bacteriol* 145:442–451. <https://doi.org/10.1128/jb.145.1.442-451.1981>.
39. Archibald FS, Duong MN. 1984. Manganese acquisition by *Lactobacillus plantarum*. *J Bacteriol* 158:1–8. <https://doi.org/10.1128/jb.158.1-1-8.1984>.
40. Ghosal D, Omelchenko MV, Gaidamakova EK, Matrosova VY, Vasilenko A, Venkateswaran A, Zhai M, Kostandarithes HM, Brim H, Makarova KS, Wackett LP, Fredrickson JK, Daly MJ. 2005. How radiation kills cells: survival of *Deinococcus radiodurans* and *Shewanella oneidensis* under oxidative stress. *FEMS Microbiol Rev* 29:361–375.
41. Sharma A, Gaidamakova EK, Matrosova VY, Bennett B, Daly MJ, Hoffman BM. 2013. Responses of Mn²⁺ speciation in *Deinococcus radiodurans* and *Escherichia coli* to γ -radiation by advanced paramagnetic resonance methods. *Proc Natl Acad Sci U S A* 110:5945–5950. <https://doi.org/10.1073/pnas.1303376110>.
42. Doonan R, McElwee JJ, Matthijssens F, Walker GA, Houthoofd K, Back P, Matscher A, Vanfleteren JR, Gems D. 2008. Against the oxidative damage theory of aging: superoxide dismutases protect against oxidative stress but have little or no effect on life span in *Caenorhabditis elegans*. *Genes Dev* 22:3236–3241. <https://doi.org/10.1101/gad.504808>.
43. Van Raamsdonk JM, Hekimi S. 2012. Superoxide dismutase is dispensable for normal animal lifespan. *Proc Natl Acad Sci U S A* 109:5785–5790. <https://doi.org/10.1073/pnas.1116158109>.
44. Fredrickson JK, Li SM, Gaidamakova EK, Matrosova VY, Zhai M, Sulloway HM, Scholten JC, Brown MG, Balkwill DL, Daly MJ. 2008. Protein oxidation:

- key to bacterial desiccation resistance? ISME J 2:393–403. <https://doi.org/10.1038/ismej.2007.116>.
45. Gupta P, Gayen M, Smith JT, Gaidamakova EK, Matrosova VY, Grichenko O, Knollmann-Ritschel B, Daly MJ, Kiang JG, Maheshwari RK. 2016. MDP: a Deinococcus Mn²⁺-decapeptide complex protects mice from ionizing radiation. PLoS One 11:e0160575. <https://doi.org/10.1371/journal.pone.0160575>.
 46. Van Raamsdonk JM, Hekimi S. 2009. Deletion of the mitochondrial superoxide dismutase sod-2 extends lifespan in *Caenorhabditis elegans*. PLoS Genet 5:e1000361. <https://doi.org/10.1371/journal.pgen.1000361>.
 47. Hastings JW, Holzapfel WH, Niemand JG. 1986. Radiation resistance of lactobacilli isolated from radurized meat relative to growth and environment. Appl Environ Microbiol 52:898–901. <https://doi.org/10.1128/aem.52.4.898-901.1986>.
 48. Levine RL, Williams JA, Stadtman ER, Shacter E. 1994. Carbonyl assays for determination of oxidatively modified proteins. Methods Enzymol 233: 346–357. [https://doi.org/10.1016/s0076-6879\(94\)33040-9](https://doi.org/10.1016/s0076-6879(94)33040-9).
 49. Das N, Levine RL, Orr WC, Sohal RS. 2001. Selectivity of protein oxidative damage during aging in *Drosophila melanogaster*. Biochem J 360: 209–216. <https://doi.org/10.1042/bj3600209>.
 50. Krisko A, Radman M. 2010. Protein damage and death by radiation in *Escherichia coli* and *Deinococcus radiodurans*. Proc Natl Acad Sci U S A 107:14373–14377. <https://doi.org/10.1073/pnas.1009312107>.
 51. Radman M. 2016. Protein damage, radiation sensitivity and aging. DNA Repair (Amst) 44:186–192. <https://doi.org/10.1016/j.dnarep.2016.05.025>.
 52. Markillie LM, Varnum SM, Hradecky P, Wong KK. 1999. Targeted mutagenesis by duplication insertion in the radioresistant bacterium *Deinococcus radiodurans*: radiation sensitivities of catalase (katA) and superoxide dismutase (sodA) mutants. J Bacteriol 181:666–669. <https://doi.org/10.1128/JB.181.2.666-669.1999>.
 53. Schaar CE, Dues DJ, Spielbauer KK, Machiela E, Cooper JF, Senchuk M, Hekimi S, Van Raamsdonk JM. 2015. Mitochondrial and cytoplasmic ROS have opposing effects on lifespan. PLoS Genet 11:e1004972. <https://doi.org/10.1371/journal.pgen.1004972>.
 54. Senchuk MM, Dues DJ, Van Raamsdonk JM. 2017. Measuring oxidative stress in *Caenorhabditis elegans*: paraquat and juglone sensitivity assays. Bio Protoc 7:e2086. <https://doi.org/10.21769/BioProtoc.2086>.
 55. Yun YS, Lee YN. 2003. Production of superoxide dismutase by *Deinococcus radiophilus*. J Biochem Mol Biol 36:282–287. <https://doi.org/10.5483/BMBRep.2003.36.3.282>.
 56. Han R, Fang J, Jiang J, Gaidamakova EK, Tkavc R, Daly MJ, Contreras LM. 2020. Signal recognition particle RNA contributes to oxidative stress response in *Deinococcus radiodurans* by modulating catalase localization. Front Microbiol 11:613571. <https://doi.org/10.3389/fmicb.2020.613571>.
 57. Erkut C, Vasilij A, Boland S, Habermann B, Shevchenko A, Kurzchalia TV. 2013. Molecular strategies of the *Caenorhabditis elegans* dauer larva to survive extreme desiccation. PLoS One 8:e82473. <https://doi.org/10.1371/journal.pone.0082473>.
 58. Wang Y, Branicky R, Noë A, Hekimi S. 2018. Superoxide dismutases: dual roles in controlling ROS damage and regulating ROS signaling. J Cell Biol 217:1915–1928. <https://doi.org/10.1083/jcb.201708007>.
 59. Gade VR, Traikov S, Oertel J, Fahmy K, Kurzchalia TV. 2020. *C. elegans* possess a general program to enter cryptobiosis that allows dauer larvae to survive different kinds of abiotic stress. Sci Rep 10:13466. <https://doi.org/10.1038/s41598-020-70311-8>.
 60. Erkut C, Kurzchalia TV. 2015. The *C. elegans* dauer larva as a paradigm to study metabolic suppression and desiccation tolerance. Planta 242: 389–396. <https://doi.org/10.1007/s00425-015-2300-x>.
 61. Puskin JS, Gunter TE. 1973. Ion and pH gradients across the transport membrane of mitochondria following Mn⁺⁺ uptake in the presence of acetate. Biochem Biophys Res Commun 51:797–803. [https://doi.org/10.1016/0006-291X\(73\)91385-5](https://doi.org/10.1016/0006-291X(73)91385-5).
 62. Gunter TE, Gavin CE, Gunter KK. 2009. The case for manganese interaction with mitochondria. Neurotoxicology 30:727–729. <https://doi.org/10.1016/j.neuro.2009.05.003>.
 63. Scott MD, Meshnick SR, Eaton JW. 1989. Superoxide dismutase amplifies organismal sensitivity to ionizing radiation. J Biol Chem 264:2498–2501. [https://doi.org/10.1016/S0021-9258\(19\)81641-1](https://doi.org/10.1016/S0021-9258(19)81641-1).
 64. Lin YT, Hoang H, Hsieh SI, Rangel N, Foster AL, Sampayo JN, Lithgow GJ, Srinivasan C. 2006. Manganous ion supplementation accelerates wild type development, enhances stress resistance, and rescues the life span of a short-lived *Caenorhabditis elegans* mutant. Free Radic Biol Med 40: 1185–1193. <https://doi.org/10.1016/j.freeradbiomed.2005.11.007>.
 65. Matsuura J, Tajima Y, Karasawa M. 1987. Metallothionein induction as a potent means of radiation protection in mice. Radiat Res 111:267–275. <https://doi.org/10.2307/3576984>.
 66. Doble PA, Miklos GLG. 2018. Distributions of manganese in diverse human cancers provide insights into tumour radioresistance. Metallomics 10:1191–1210. <https://doi.org/10.1039/c8mt00110c>.
 67. Pérez VI, Bokov A, Van Remmen H, Mele J, Ran Q, Ikono Y, Richardson A. 2009. Is the oxidative stress theory of aging dead? Biochim Biophys Acta 1790:1005–1014. <https://doi.org/10.1016/j.bbagen.2009.06.003>.
 68. Salmon AB, Richardson A, Pérez VI. 2010. Update on the oxidative stress theory of aging: does oxidative stress play a role in aging or healthy aging? Free Radic Biol Med 48:642–655. <https://doi.org/10.1016/j.freeradbiomed.2009.12.015>.
 69. Munkácsy E, Rea SL. 2014. The paradox of mitochondrial dysfunction and extended longevity. Exp Gerontol 56:221–233. <https://doi.org/10.1016/j.exger.2014.03.016>.
 70. Daly MJ, Ouyang L, Fuchs P, Minton KW. 1994. In vivo damage and recA-dependent repair of plasmid and chromosomal DNA in the radiation-resistant bacterium *Deinococcus radiodurans*. J Bacteriol 176:3508–3517. <https://doi.org/10.1128/jb.176.12.3508-3517.1994>.
 71. Daly MJ, Minton KW. 1996. An alternative pathway of recombination of chromosomal fragments precedes recA-dependent recombination in the radioresistant bacterium *Deinococcus radiodurans*. J Bacteriol 178: 4461–4471. <https://doi.org/10.1128/jb.178.15.4461-4471.1996>.
 72. Nass R, Hamza I. 2007. The nematode *C. elegans* as an animal model to explore toxicology in vivo: solid and axenic growth culture conditions and compound exposure parameters. Curr Protoc Toxicol Chapter 1:Unit1.9. <https://doi.org/10.1002/0471140856.tx0109s31>.
 73. Szewczyk NJ, Kozak E, Conley CA. 2003. Chemically defined medium and *Caenorhabditis elegans*. BMC Biotechnol 3:19. <https://doi.org/10.1186/1472-6750-3-19>.
 74. Flavel MR, Mechler A, Shahmiri M, Mathews ER, Franks AE, Chen W, Zanker D, Xian B, Gao S, Luo J, Tegegne S, Doneski C, Jois M. 2018. Growth of *Caenorhabditis elegans* in defined media is dependent on presence of particulate matter. G3 (Bethesda) 8:567–575. <https://doi.org/10.1534/g3.117.300325>.
 75. Werst MM, Davoust CE, Hoffman BM. 1991. Ligand spin densities in blue copper proteins by q-band proton and nitrogen-14 ENDOR spectroscopy. J Am Chem Soc 113:1533–1538. <https://doi.org/10.1021/ja00005a011>.
 76. Tsednee M, Castruita M, Salomé PA, Sharma A, Lewis BE, Schmollinger SR, Strenkert D, Holbrook K, Otegui MS, Khatua K, Das S, Datta A, Chen S, Ramon C, Ralle M, Weber PK, Stemmler TL, Pett-Ridge J, Hoffman BM, Merchant SS. 2019. Manganese co-localizes with calcium and phosphorus in *Chlamydomonas acidocalcisomes* and is mobilized in manganese-deficient conditions. J Biol Chem 294:17626–17641. <https://doi.org/10.1074/jbc.RA119.009130>.